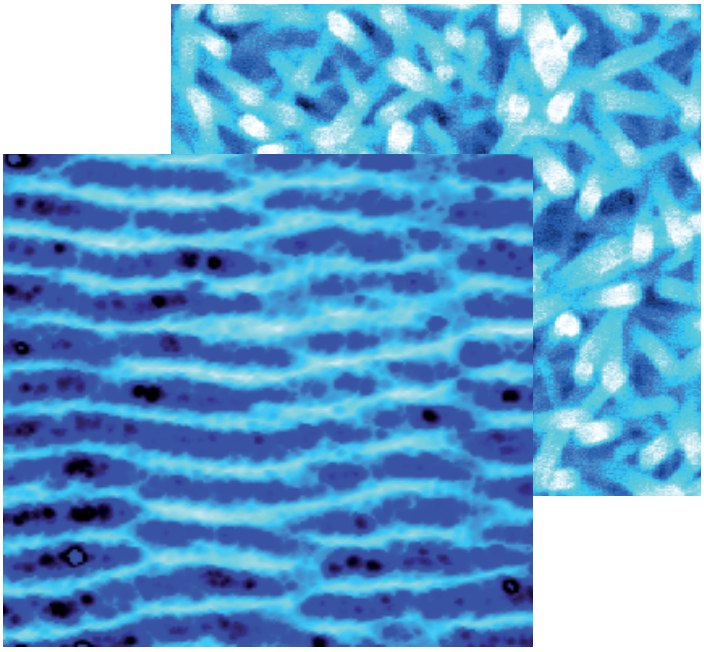

Book of Abstracts

2nd International Workshop on

Nonlinear Nanostructures for Ultrafast Laser Applications

May 19 - 20, 2011

Max Born Institute

Table of Contents

Scope of the workshop 3

Program Committee - Sponsors 4

Scientific Program ..... 5 - 8

Abstracts of Talks ..... 9 - 34

Focus Session „Laser-Induced Nanostructures“

1. Nanostructure formation at metal surfaces ..... 9 - 11
2. General aspects and structuring in three dimensions ..... 12 - 14
3. Nanostructure formation in semiconductors and dielectrics ..... 15 - 18

Focus Session „Nonlinear Nanooptics“

4. Plasmonics, metamaterials and nonlinear optics ..... 19 - 28
5. Spectroscopy, gain materials and characterization ..... 29 - 34

Abstracts of Posters ..... 35 - 44

Author Index ..... 45 - 46

Scope of the workshop

Ultrashort laser pulses have developed into an important tool for structuring materials on a micro- and nanometer scale. In parallel, nanomaterials find increasing application in nonlinear optics, plasmonics, and light generation. Most recent results in such areas are presented at the 2nd International Workshop on Nonlinear Nanostructures for Ultrafast Laser Applications. The scientific program is comprised of 21 oral and 8 poster contributions which are complemented by lab tours and presentations by companies. More than 120 authors from 10 countries are contributing to the event, a substantial increase compared to the first workshop which was held in 2009. A significant fraction of contributions will be presented by young scientists. The meeting is intended to develop into a major platform for discussing new results, exchanging ideas, and developing new projects in a truly interdisciplinary field.

The organizers would like to express their gratitude to the sponsors of the workshop. Their generous support allows for running the meeting smoothly and without raising a conference fee from the participants. We enjoy to host the event at the Max-Born-Institute and wish all participants a successful workshop.

Rüdiger Grunwald
for the organizing committee

Program Committee

Prof. Thomas Elsaesser
(Max-Born-Institute, Berlin, Germany)

Prof. Peter R. Herman
(University of Toronto, Canada)

Prof. Peter G. Kazansky
(ORC, University of Southampton, UK)

Prof. Christoph Lienau
(University Oldenburg, Germany)

Prof. Gerd Marowsky
(Laser Laboratory Göttingen, Germany

Sponsors

Laserlab Europe

lehmanns media

A P E

OpTecBB

MBI Max-Born-Institut

HOLOEYE

Forschungsverbund Berlin e.V.

JCMwave

LightTrans

Local Organizing Committee & Administrative Support

Dr. R. Grunwald
M. Lehmann
J. Michel
C. Reschke
D. Stozno
Dr. B. Weidner
S. Wende
A. Wettstein

Address:

MBI Max-Born-Institute for Nonlinear Optics and Short Pulse Spectroscopy im Forschungsverbund Berlin e.V.
Max-Born-Straße 2A - 12489 Berlin-Adlershof
Telephone: +49 (0)30 6392 1402 - Telefax: +49 (0)30 6392 1409
Email: MBI-NANO-2011@mbi-berlin.de - Website: www.mbi-berlin.de & www.laserlab-europe.eu

Conception & Layout:
Alexandra Wettstein - email: alexandra.wettstein@mbi-berlin.de

Scientific Program

Thursday, May 19, 2011

08:00 - 11:00 **Registration and Information**
09:00 - 09:15 **Welcome**

Focus Session „LASER-INDUCED NANOSTRUCTURES“

1. Nanostructure formation at metal surfaces

09:15 - 10:15 **Scaling law of grating interspace for self-formed periodic structures on a metal surface by femtosecond laser pulses** (keynote lecture)
S. Sakabe, M. Hashida, S. Tokita, Y. Miyasaka, and Y. Ikuta

10:15 - 10:45 **Femtosecond laser nano-ablation processes of metals discussed with ablation rate, ablated-ion spectroscopy, and crystal structures**
M. Hashida, Y. Miyasaka, Y. Ikuta, S. Tokita, and S. Sakabe

10:45 - 11:00 **Coffee Break**

2. General aspects and structuring in three dimensions

11:00 - 11:45 **Self-organized nano-structure formation upon femtosecond laser ablation** (invited)
J. Reif, O. Varlamova, M. Bounhalli, M. Muth, S. Varlamov, and M. Bestehorn

11:45 - 12:30 **Harnessing ultrafast laser induced nanostructures in transparent materials** (invited)
P. G. Kazansky, M. Beresna, and M. Gecevičius

12:30 - 13:45 **Lunch**

3. Nanostructure formation in semiconductors and dielectrics

13:45 - 14:30 **Formation process of femtosecond laser-induced nanogratings in fused silica at high repetition rates**
S. Richter, S. Döring, A. Tünnermann, and S. Nolte

14:30 - 15:00 **Review on parameters controlling the formation of laser induced periodic structures in TiO_2 single crystal and thin films**
S.K. Das, A. Rosenfeld, J. O. Bonse, A. Pfuch, W. Seeber, and R. Grunwald

15:00 - 15:15 **Coffee Break**

15:15 - 15:45 **Formation of laser-induced periodic surface structures on dielectrics and semiconductors upon double-femtosecond laser pulse irradiation sequences**
S. Höhm, M. Rohloff, J. Krüger, J. O. Bonse, and A. Rosenfeld

16:00 - 17:30 **Lab Visits at the Max-Born-Institute**

17:30 - 18:00 **Poster Session**

Poster 1 **Characteristics of ions emitted from the nano-ablation processes with femtosecond laser pulses of the fluence near ablation threshold**
Y. Miyasaka, M. Hashida, Y. Ikuta, S. Tokita, and S. Sakabe

Poster 2 **3D active photonic nanostructures**
E. A. Kabouraki, I. Sakellari, C. Fotakis, M. Vamvakaki, and M. Farsari

Poster 3 **Enhanced third order nonlinearity in nanocrystalline TiO_2 thin films,**
S.K. Das, C.Schwanke, M. Bock, A. Pfuch, W. Seeber, and R. Grunwald

Poster 4 **Compact and tunable sub-20 fs laser source for ultrafast nonlinear applications**
B. Metzger, A. Steinmann, G. Albrecht, and H. Giessen

Poster 5 **Germanium nanowire growth**
R. Bansen, J. Schmidtbauer, T. Teubner, H.P. Schramm, and T. Boeck

Poster 6 **Studies of bound exciton and surface excitonic emissions in nanostructured and bulk ZnO**
M. Biswas, K. Kumar, G. Hughes, D. McCabe, K. Johnston, Marc Dietrich, E. Alves, M. Xia, E. McGlynn, and M. O. Henry

Poster 7 **Nano-indentation study of femtosecond laser induced periodic surface structures on dielectrics and semiconductors**
M. Rohloff, A. Richter, K. Dasari, R. Hertmanowski, S. K. Das, A. Rosenfeld, and R. Grunwald

Poster 8 **Ultrafast electron dynamics in ZnO/Si micro-cones**
E. Magoulakis, E. L. Papadopoulou, E. Stratakis, C. Fotakis, and P. A. Loukakos,

Poster presentations of companies

Poster 9 HoloEye Photonics AG, Presentation of the company
Poster 10 LightTrans GmbH, Presentation of the company
Poster 11 APE GmbH, Presentation of the company

Product presentations of companies

M. Kuhn **LightTrans GmbH, Field Tracing Software VirtualLab™**
H. Bethmann **Lehmanns Fachbuchhandlung, Scientific Books**

M. Kuhn, LightTrans GmbH, Field Tracing Software VirtualLab™

18:00 - 20:00 **Get-together at Max-Born-Hall**

08:00 - 11:00 **Registration and Information**

Focus Session „NONLINEAR NANOOPTICS“

4. Plasmonics, metamaterials and nonlinear optics

08:30 - 09:15 **Coupling surface plasmon polaritons to excitons in metal-j-aggregate hybrid nanostructures** (invited)
P. Vasa, R. Pomraenke, W. Wang, M. Lammers, M. Maiuri, C. Manzoni, G. Cerullo, and C. Lienau

09:15 - 09:35 **Direct laser writing of gain and metallic nanostructures**
I. Sakellari, E. A. Kabouraki, V. Purlys, A. Gaidukeviciute, D. Gray, C. Fotakis, M. Vamvakaki, and M. Farsari

09:35 - 09:55 **Towards unraveling the mechanism of third harmonic generation in plasmonic nanoantennas**
M. Hentschel, T. Utikal, M. Lippitz, and H. Giessen

09:55 - 10:15 **Strong field photoemission from metal nanotips**
M. Gulde, R. Bormann, S. V. Yalunin, A. Weismann, and C. Ropers

10:15 - 10:30 **Coffee Break**

10:30 - 10:50 **Theory of low-threshold high-order harmonic generation by using field enhancement near metallic fractal surfaces**
K.-H. Kim, A. Husakou, and J. Herrmann

10:50 - 11:10 **Optical Harmonic Generation in bow tie nanoantennas**
M. Sivis, M. Duwe, K. R. Siefermann, Y. Liu, B. Abel, and C. Ropers

11:10 - 11:30 **Weak localization of light in ZnO nanorods in space and time**
M. Maschek, S. Schmidt, M. Silies, C. Lienau, D. Leipold, E. Runge, T. Yatsui, K. Kitamura, and M. Ohtsu

11:30 - 12:00 **Finite-element method simulations of plasmonic devices and materials**
S. Burger

12:00 - 12:20 **Broadband (~1000 nm) carbon nanotube saturable absorber mode-locking of bulk solid-state lasers**
A. Schmidt, G. Steinmeyer, V. Petrov, U. Griebner, S.Y. Choi, W.B. Cho, D.-I. Yeom, K. Kim, and F. Rotermund

12:20 - 13:30 **Lunch**

5. Spectroscopy, gain materials and characterization

13:30 - 13:50 **Ultrafast electron transport suppression in Au nanowire networks**
E. Magoulakis, A. Kostopoulou, C. Brintakis, A. Andriotis, A. G. Kanaras, A. Lappas, and P. A. Loukakos

13:50 - 14:10 **Time-resolved microscopy of fs laser-induced refractive index modifications in the volume of a-SiO2**
A. Mermillod-Blondin, C. Mauclair, A. Rosenfeld, J. Bonse, R. Stoian, and E. Audouard

14:10 - 14:30 **Determination of the photoluminescence quantum efficiency of silicon nano-crystals by laser-induced deflection**
W. Paa, Ch. Mühlig, K. Potrick, T. Schmidt, S. Bublitz, and F. Huisken

14:30 - 14:45 **Coffee break**

14:45 - 15:05 **Real-space distribution of cavity modes in single ZnO nanowires**
F. Güell, A. R. Goñi, J. O. Ossó, L. A. Pérez, E. A. Coronado, A. Cornet, and J. R. Morante

15:05 - 15:25 **Local nano-structure and morphology of organic thin films**
S. Kühn

15:25 - 15:30 **Closing remarks (Organizers)**

15:45 - 17:00 **Lab Visits at the Leibniz Institute for Crystal Growth**

Abstracts of Talks

Focus Session „LASER-INDUCED NANOSTRUCTURES“

1. **Nanostructure formation at metal surfaces**
2. General aspects and structuring in three dimensions
3. Nanostructure formation in semiconductors and dielectrics

Focus Session „NONLINEAR NANOOPTICS“

4. Plasmonics, metamaterials and nonlinear optics
5. Spectroscopy, gain materials and characterization

Scaling Law of Grating Interspace for Self-Formed Periodic Structures on a Metal Surface by Femtosecond Laser Pulses

Shuji Sakabe

Co-workers: Masaki Hashida, Shigeki Tokita, Yasuhiro Miyasaka, and Yoshinobu Ikuta

Advanced Reserach Center for Beam Science, Institute for Chemical Research, Kyoto University, Gokasho, Uji, Kyoto 611-0011, Japna

and Department of Physics, Graduate School of Science, Kyoto University, Kitashirakawa, Sakyo, Kyoto 606-7501, Japan

E-mail address : sakabe@laser.kuicr.kyoto-u.ac.jp

Since the self-formation of periodic structures in or on insulators, semiconductors, and metals by the irradiation of femtosecond laser pulses were found concurrently with one another but independently, the characteristics and future applications have been intensively studied. Such structures on matter are named LIPSS (Laser Induced Periodic Structure on Surface). Hashida *et al*. has reported the observation of the LIPSS on a copper surface and measured the dependence of LIPSS interspace on laser fluence, using 800nm femtosecond lasers [1, 2]. The dependence (Fig.1) shows the following features: (1) The interspace depends on laser fluence, (2) there is the upper limit for fluence to form LIPSS, (3) the maximum interspace is 700nm, and it is not as long as, but less than laser wavelength, (3) the maximum interspace is formed at the upper limit fluence, (4) the interspaces become shorter in a discontinuous manner at near the ablation threshold as the laser fluence decreases. The physical mechanism of LIPSS is not well interpreted as affairs now stand, and still under investigation. We are currently studying the mechanism with a hypothesis that the periodic structure patterns are initially printed and ablated by the latter part of a pulse or following pulses, keeping the initial printed patterns as they are. We have considered the initial printing would be driven by laser induced plasma waves, and presented an interpretation for the interspaces of LIPSS on metals [3]. For femtosecond-pulse laser matter interactions, the scale length of laser produced plasma at the abration front during the laser pulse is short enough for the plasma to form a clear surface (discontinuous steep density change). On such a surface the surface plasma waves would be excited. However the direct excitation by the incident laser cannot produce the plasma wave of which wavelength is as short as the interspace of LIPSS. We have proposed a parametric process for the laser light to be decayed into the surface plasma wave and light, which is in general called Stimulated Raman Scattering for bulk plasmas. In this process the wavelength of the plasma wave depends on plasma frequency (density), which changes with laser fluence, resulting in the laser fluence dependence of LIPSS interspace. The solid line in Fig.1 is obtained by the calculation with this mechanism for initial printing, and it is in fairly good agreement with the experimental results. Universality of the present interpretation for LIPSS interspace has been confirmed by studying the LIPPS formed for several kinds of metals [4] or using SHG light pulses, and the measured fluence scaling laws of interspace are well reproduced by the present interpretation.

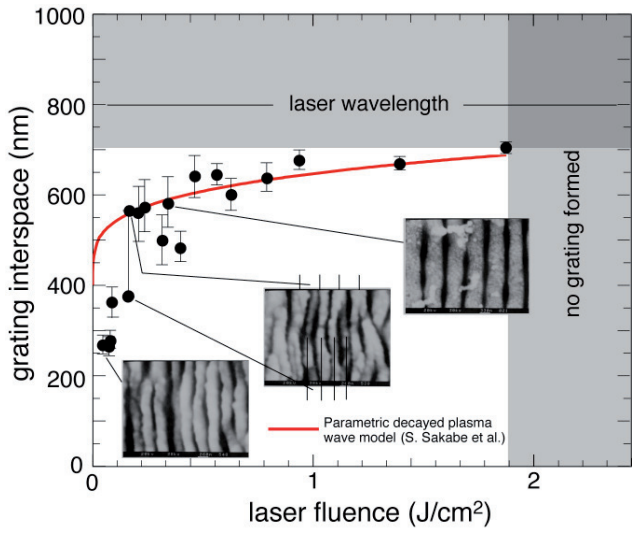

Fig. 1 The dependence of the LIPSS grating interspace on laser fluence, and (inset) the SEM pictures of LIPSS seen on the laser-ablated metal surface. The metal sample is a mechanically polished copper plate. The LIPSS was produced by 100-fs, 800-nm laser pulses. The Laser pulses are irradiated on the copper plate in normal direction through a lens, and scanned on the surface. The solid line is the wavelength of surface plasma wave induced by parametric decay of laser light.

This work was partially supported by the Grant-in-Aid for the Global COE Program "The Next Generation of Physics, Spun from Universality and Emergence" from the Ministry of Education, Culture, Sports, Science and Technology (MEXT) of Japan.

References

[1] M. Hashida, *et al*, in *Laser Precision Microfabrication*, Proceedings of SPIE, ed. by I. Miyamoto *et al.* (SPIE, Washington), Vol.4830, pp.452-457(2002).; M. Hashida, *et al*., in Nonresonant Laser-Matter Interaction (NLMI-10), Proceedings of SPIE , ed. by M. N. Libenson (SPIE, Washington, 2001), Vol.4423. pp.178-185.

[2] M. Hashida, *et al*., Appl. Surf. Sci. **197-198**, 826(2002).

[3] S. Sakabe, *et al*., Phys. Rev B **79**, 033409(2009).

[4] K. Okamuro, *et al*., Phys. Rev. B **82**, 165417(2010).

Femtosecond laser nano-ablation processes of metals discussed with ablation rate, ablated-ion spectroscopy, and crystal structures

Masaki Hashida, Yasuhiro Miyasaka, Yoshinobu Ikuta, Shigeki Tokita, and Shuji Sakabe

Advanced Research Center for Beam Science, Institute for Chemical Research, Kyoto University, Gokasho, Uji, Kyoto 611-0011, Japan and Department of Physics, Graduate School of Science, Kyoto University, Kitashirakawa, Sakyo, Kyoto 606-8502, Japan

For the single crystalline copper film of which surface is periodically self-structured by femtosecond laser pulses in the laser fluence of 0.08~0.64 J/cm^2, crystal structures have been analyzed by transmission electron microscopy. It was found that the crystal structures are transformed depending on laser fluence; polycrystalline structures at < 0.2 J/cm^2, amorphous at ~0.3 J/cm^2, and polycrystalline structures again at > 0.35 J/cm^2. The energy spectroscopic study of ions emitted [1] during the self-formation of periodic structures [2][3] on the surface shows the energy of copper ions is reasonable high enough to transform the crystal to an amorphous state. The mechanism of crystal structure transformation by femtosecond laser pulses is conceptually proposed, that is induced by the injection of energetic ions generated in the process of self-formation of periodic structures.

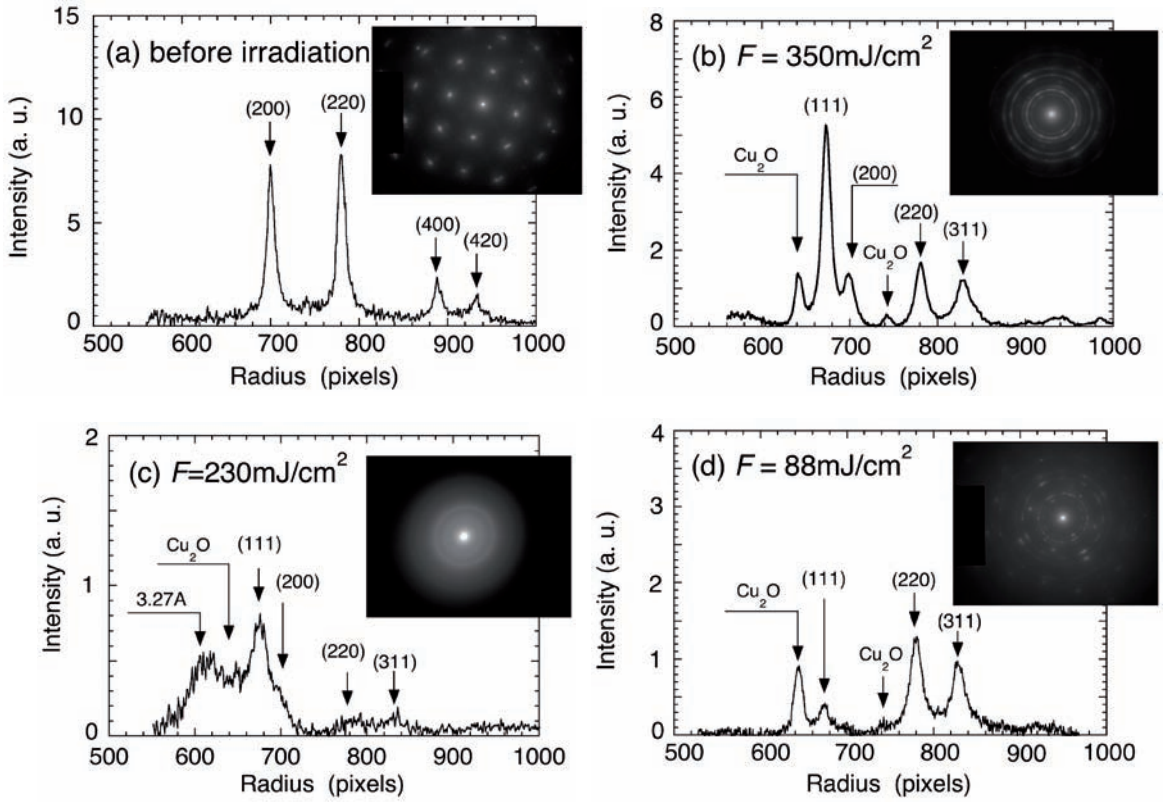

Fig. 1. Electron diffraction patterns of thin Cu films (a) before irradiation, (b) at 0.35 J/cm^2, (c) at 0.23 J/cm^2, and (d) at 0.088 J/cm^2.

[1]M. Hashida el al. Phys Rev B **81**(2010)115442.
[2] S. Okamuro et al. Phys. Rev B **82**(2010)165417.
[3] S. Sakabe et. al. Phys. Rev. B **79**(2009) 033409.

Abstracts of Talks

Focus Session „LASER-INDUCED NANOSTRUCTURES“

1. Nanostructures formation at metal surfaces
2. **General aspects and structuring in three dimensions**
3. Nanostructure formation in semiconductors and dielectrics

Focus Session „NONLINEAR NANOOPTICS“

4. Plasmonics, metamaterials and nonlinear optics
5. Spectroscopy, gain materials and characterization

Self-organized nano-structure formation upon femtosecond laser ablation

J. Reif, O. Varlamova, M. Bounhalli, M. Muth, S. Varlamov, M. Bestehorn
Brandenburgische Technische Universitaet (BTU) Cottbus, Germany

Self-organized nanostructures (ripples) developing at the surface of all types of materials upon femtosecond laser ablation exhibit, a strong influence of the laser polarization on their orientation and shape. This dependence is very surprising, taking into account that the laser electric field is present only at the first step of electronic excitation. During particle emission (ablation) and subsequent structure formation, the laser field is NOT present.
We present a theoretical model and corresponding simulations indicating a possible explanation for this phenomenon. Basically, it describes the time evolution of surface corrugation as a competition of surface erosion and surface smoothing due to diffusion. We show that a spatial anisotropy already during the absorption of the laser pulses may result in a directional anisotropy for the pattern generation. This anisotropy might, e.g. be due to a polarization dependent coupling to transient surface plasmons/polaritons or to an anisotropic kinetic energy distribution of the photoionized electrons.
Numerical simulation of the consequences of this model yields typical patterns which can be compared to experimental observations under appropriate conditions (Fig. 1).

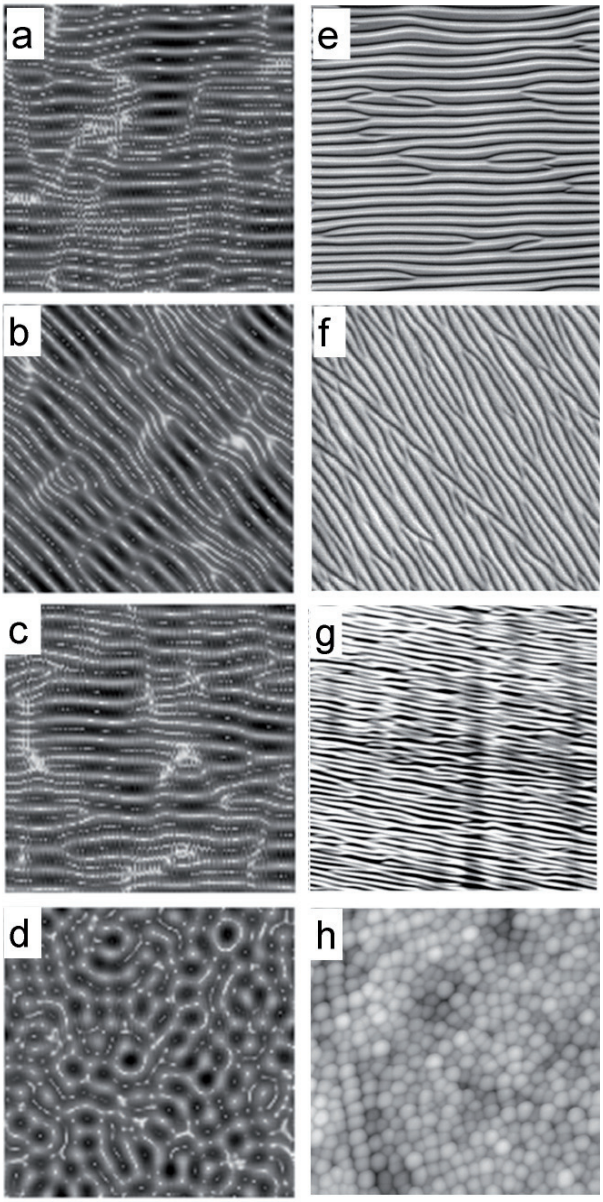

Figure 1: Comparison between simulation (left) and experimental results (right).

Further, we studied the effect of double laser pulses with a separation between one pulse width (100 fs) and a few picoseconds. Similar to earlier observations on the ablation *efficiency*, we find a significant impact for delays of some tens of picoseconds.
The increase of ablation yield as well as a coarsening of structure formation occurs essentially in the outer regions of the irradiated spot, whereas at the center the total ablation depth decreases with increasing pulse separation, showing only structures usually observed for low irradiation. The nanostructures modulation oscillates between elevation above and depression below the unaffected surface level. Micro-Raman spectroscopy of the modified areas indicates an unexpectedly high abundance of very confined nanostructures.

Harnessing Ultrafast Laser Induced Nanostructures in Transparent Materials

***P. G. Kazansky, M. Beresna and M.* Gecevičius**

Optoelectronics Research Centre, University of Southampton, SO171BJ Southampton, UK

Material processing with ultrafast lasers has attracted considerable interest due to a wide range of applications from laser surgery and integrated optics to optical data storage, 3D micro- and nano-structuring [1,2]. A decade ago it has been discovered that under certain irradiation conditions ordered sub-wavelength structures with features smaller than 20 nm can be formed in the volume of silica glass [3]. The effect of nanograting formation has attracted considerable interest with proposals of applications ranging from nanofluidics [4,5] to polarization control devices [6].

More recently, the self-assembled sub-wavelength nanostructuring have been proposed for fabrication of vortex polarization converters (Fig. 1) and rewritable polarization multiplexed optical memory [7], where the information encoding is realized by means of two birefringence parameters, i.e. the slow axis orientation (4th dimension) and retardance (5th dimension), in addition to three spatial coordinates (Fig.2).

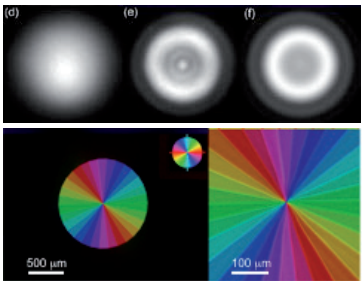

Fig. 1 Measured beam profiles of argon ion cw laser befor, after radially polarized vortex beam converter and modelled beam profile after beam converter (top). Color-coded distribution of slow axis measured with Abrio system (bottom).

Fig. 2 | Ultrafast optical recording via self-assembled nanograting induced birefringence in fused silica. Maxwell and Newton are recorded in one image (left, in pseudo colours), however, they can be easily decoupled as Maxwell is recorded in strength of retardance (centre) and Newton in azimuth of the slow axis (right).

A remarkable effect has also been discovered, referred to as quill or calligraphic laser writing, which reveals strong dependence of the material modification, in particular the self-assembled sub-wavelength structures in glass, on orientation of the writing direction relative to direction of the pulse front tilt [8-10]. Moreover, evidence of the first order phase transition associated with self-assembled nanostructures formation was revealed and supercooled state of laser damage was observed using pulses with tilted intensity front. More recently it has been demonstrated that the tip of an ultrafast laser quill has a property that is very different from an ordinary quill [11]. Specifically, the modification of glass can be controlled even in stationary conditions by the mutual orientation of light polarization azimuth and the pulse front tilt. Figuratively, the polarization can be used as a sharpening blade for the ultrafast light quill. The demonstrations of self-assembled nano-structuring and employing mutual orientations of beam movement or the light polarization plane and pulse front tilt to control interaction of matter with ultrashort light pulses, open new opportunities in material processing.

References

[1] R. R. Gattas and E. Mazur, “Femtosecond laser micromachining in transparent materials,” Nature Photonics **2**, 219 (2008).
[2] W. Yang, P. G. Kazansky, and Yu. P. Svirko, “Non-reciprocal ultrafast laser writing,” Nature Photonics **2**, 99 (2008).
[3] Y. Shimotsuma, P. G. Kazansky, J. Qiu, and K. Hirao, “Self-organized nanogratings in glass irradiated by ultrashort light pulses,” Phys. Rev. Lett. **91**, 247705 (2003).
[4] Y. Bellouard, A. Said, M. Dugan, and P. Bado, "Fabrication of high-aspect ratio, micro-fluidic channels and tunnels using femtosecond laser pulses and chemical etching," Opt. Express **12**, 2120 (2004).
[5] V. Bhardwaj, E. Simova, P. Rajeev, C. Hnatovsky, R. Taylor, D. Rayner, and P. Corkum, “Optically produced arrays of planar nanostructures inside fused silica,” Phys. Rev. Lett. **96**, 057404-1 (2006).
[6] M. Beresna and P. G. Kazansky, "Polarization diffraction grating produced by femtosecond laser nanostructuring in glass," Opt. Lett. **35**, 1662 (2010).
[7] Y. Shimotsuma *et. al.,* “Ultrafast manipulation of self-assembled form birefringence in glass,”Advanced Materials **22** (36), 4039 (2010).
[8] P. G. Kazansky *et al.,* “Quill" writing with ultrashort light pulses in transparent materials,” Appl. Phys. Lett. **90**, 151120 (2007).
[9] B. Poumellec *et al*., “Non reciprocal writing and chirality in femtosecond laser irradiated silica,” Opt. Express 16, 18354 (2008).
[10] D. N. Vitek, E. Block, Y. Bellouard, D. E. Adams, S. Backus, D. Kleinfeld, C. G. Durfee, and J. A. Squier, “Spatio-temporally focused femtosecond laser pulses for nonreciprocal writing in optically transparent materials,” Opt. Express **18**, 24673 (2010).
[11] P. G. Kazansky *et al*., “Polarization control of ultrafast laser writing using pulses with tilted front”, submitted to Phys. Rev. Lett. (2011).

Abstracts of Talks

Focus Session „LASER-INDUCED NANOSTRUCTURES“

1. Nanostructure formation at metal surfaces
2. General aspects and structuring in three dimensions
3. **Nanostructure formation in semiconductors and dielectrics**

Focus Session „NONLINEAR NANOOPTICS“

4. Plasmonics, metamaterials and nonlinear optics
5. Spectroscopy, gain materials and characterization

Formation process of Femtosecond Laser-induced Nanogratings in Fused Silica at High Repetition Rates

***S. Richter*[1], *S. Döring*[1], *A. Tünnermann*[1,2], *S. Nolte*[1,2]**

1. Friedrich-Schiller-Universität Jena, Institute of Applied Physics, Albert-Einstein- Straße 15, 07743 Jena, Germany

2. Fraunhofer Institute for Applied Optics and Precision Engineering, Albert-Einstein-Straße 7, 07745 Jena, Germany

We investigate the formation of nanogratings in fused silica induced by femtosecond laser pulses. In general, the formation of regular and periodic nanogratings occurs within a well defined range of processing parameters; see Figure 1 a). The lower limit of the formation of nanogratings is given by the minimal pulse energy to achieve nanostructures at all. The maximal applicable average laser power for the formation of nanograting is given by heat accumulation of successive pulses at high repetition rates and the accompanied homogenous melting of the material. This defines the upper limit for the nanograting formation. Consequently, the maximum usable pulse energy is inversely proportional to the repetition rate R, as the heat accumulation within material is controlled by the laser average power. Thus, by adapting the pulse energy we could significantly expand the processing window for the formation of nanogratings up to a repetition rate R of 9.4 MHz.
Furthermore, we could identify three distinct development stages from randomly arranged nanostructures to uniform periodic gratings; see fig. 1 b). These stages of the formation process are controlled mainly by the number of pulses incident on the sample. During the first formation stage, the laser exposed volume contains nonperiodic modifications with an irregular shape. Stage II is reached after several hundred pulses. Here, there are still a lot of vacancies between the isolated modifications, but periodicity starts to emerge. In stage III, which occurs after roughly 1,000 pulses, the vacancies have been filled and a periodic nanograting is formed. A further increase of the number of pulses results in a decrease of the period of the nanogratings, according to previous measurements [1].

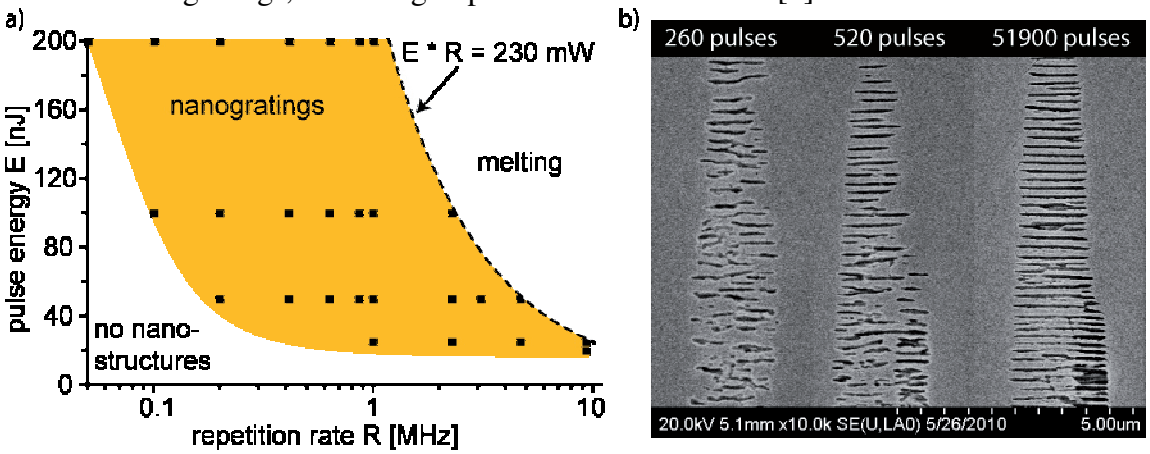

Fig. 1 a) The type of material modifications within fused silica is determined by the applied pulse energy and repetition rate. The black points are measured points were we observed the formation of nanogratings (grey area). b) Evolution of disordered nanostructures to regular nanogratings with respect to the number of applied pulses. The nanostructures were obtained while using 450 fs pulses at a wavelength of 515 nm, a repetition rate of 865 kHz and pulse energy of 150 nJ.

In agreement with the nanoplasmonic model for the formation of nanogratings [2], the number of pulses required for each formation stage depends slightly on the applied pulse energy E. Therefore, for a fixed number of pulses the period also decreases with increasing pulse energy. At higher pulse energies stage III of the formation process is reached at a smaller pulse number, and thus the decrease of the grating period has progressed further. However, in contrast to the prediction of the nanoplasmonic model we could obtain periods as low as 150 nm with a wavelength of 515 nm, which is significantly smaller than the expected $\lambda/2n$.

References

[1] L.P.Ramirez, M. Heinrich, S. Richer, F. Dreisow, R. Keil, A. V. Korovin, U. Peschel, S. Nolte, A. Tünnermann, "Tuning the structural properties of femtosecond-laser-.induced nanogratings," Appl. Pys. A, **100**, 1 (2010)

[2] R. Taylor, C. Hnatovsky, E. Simova, "Applications of femtosecond laser induced self-organized planar nanocracks inside fused silica glass," Laser Photon. Rev. **2**, 26 (2008).

Review on parameters controlling the formation of laser induced periodic structures in TiO_2 single crystals and thin films

S. K. Das[1], A. Rosenfeld[1], J. O. Bonse[2], A. Pfuch[3,4], W. Seeber[4], and R. Grunwald[1]

[1]*Max Born Institute for Nonlinear Optics and Short-Pulse Spectroscopy, Max-Born-Strasse 2a, D-12489 Berlin, Germany*
[2]*BAM Bundesanstalt für Materialforschung und -prüfung, Unter den Eichen 87, D-12205Berlin, Germany*
[3]*INNOVENT e.V., Prüssingstraße 27 B, D-07745 Jena, Germany*
[4]*Friedrich-Schiller-Universität Jena, Otto-Schott-Institut, Fraunhoferstr. 6, D-07743 Jena, Germany*

The formation of ripple-like laser induced periodic surface structures (LIPSS) is governed by a few key parameters. The complex interplay of these parameters is not fully understood, in particular for intense excitation with ultrashort pulses which enables to generate feature sizes far below the wavelength. Here we report on progress in this field with respect to specific nonlinear channels and initial conditions. The formative influence of wavelength, pulse energy and further control parameters on the LIPSS morphology in TiO_2 single crystals and thin film surfaces is discussed. It will be shown that the transient optical behaviour due to multi-photon absorption induced free carriers is of essential influence. With fs-pulses at 400 nm (frequency doubled Ti:sapphire laser), high and low spatial frequency LIPSS (HSFL, LSFL) were obtained [1]. To elucidate the pulse-to-pulse evolution and intra-pulse dynamics of ripple generation, experiments with varying pulse numbers and double pulses were performed. Because of its importance for controlling the ripple formation, scattering during the first few pulses was analysed. It was found that in the case of smooth surfaces (rms roughness 0.2 nm) the role of the initial few pulses is to generate secondary scattering centres supporting LIPSS formation with increasing pulse number [1,2]. Therefore, smooth surfaces require more pulses for shaping distinct LIPSS. If the pulse number exceeds an optimum value, however, one ends up with rather quasi-periodic structures [2]. To achieve a controlled geometry, a careful multi-parametric optimization is required. Figure 1 shows an example of an HSFL generated on a TiO_2 single crystal with 40 pulses (fluence 0.75 J/cm^2, intensity 5 x 10^{12} W/cm^2, pulse duration 150 fs, central wavelength 800 nm). The earlier appearance of ripples in the presence of scattering centres was confirmed in recent experiments [3,4] where fairly good periodic structures were found even for pulse numbers between 5 and 20.

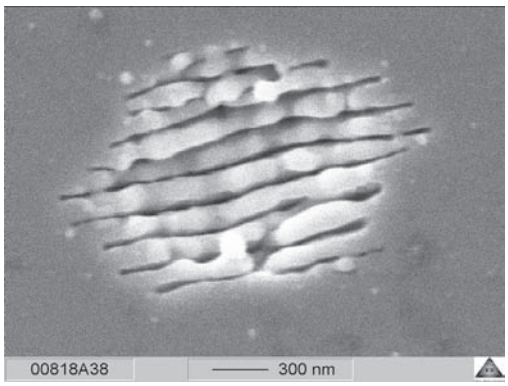

Figure 1: High spatial frequency laser-induced ripples generated in a TiO_2 single crystal surface with fs pulses at 800 nm (pulse duration 150 fs, N = 40 pulses, peak intensity 5 x 10^{12} W/cm^2).

References:

1. S. K. Das, K. Dasari, A. Rosenfeld, and R. Grunwald, Nanotechnology **21**, 155302 (2010).
2. S. K. Das, D. Dufft, A. Rosenfeld, J. Bonse, M. Bock, and R. Grunwald, J. Appl. Phys. **105**, 084912 (2009).
3. S. K. Das, M. Rohloff, A. Pfuch, W. Seeber, A. Rosenfeld, and R. Grunwald, CLEO 2011, Baltimore, USA (2011) (accepted).
4. S. K. Das, A. Rosenfeld, M. Bock, A. Pfuch, W. Seeber, and R. Grunwald, Scattering-controlled femtosecond-laser induced nanostructuring of TiO_2 thin films, Proc. SPIE **7925**-42 (2011).

Formation of laser-induced periodic surface structures on dielectrics and semiconductors upon double-femtosecond laser pulse irradiation sequences

S. Höhm[1], M. Rohloff[1], J. Krüger[2], J. Bonse[2], A. Rosenfeld[1]

[1] Max-Born-Institut, Max-Born-Straße 2a, D-12489 Berlin, Germany
[2] BAM Bundesanstalt für Materialforschung und -prüfung,
Unter den Eichen 87, D-12205 Berlin, Germany

The formation of laser-induced periodic surface structures (LIPSS) upon irradiation of dielectrics and semiconductors with multiple (N_{DPS}) irradiation sequences consisting of Ti:sapphire femtosecond laser pulse pairs (pulse duration ~150 fs, central wavelength ~800 nm) is studied experimentally. A Michelson interferometer is used to generate nearly equal-energy double-pulse sequences allowing the temporal pulse delay Δt between the equally or cross-polarized individual fs laser pulses to be varied from -30 to +30 ps with a resolution of ~0.2 ps. The results of multiple double-pulse irradiation sequences are characterized by scanning electron (SEM) and scanning force microscopy (SFM). Specifically in the sub-ps delay range striking differences in the orientation of the LIPSS and their spatial periods can be observed for dielectrics, indicating the importance of the laser-induced free-electron plasma in the conduction band for the formation of LIPSS.

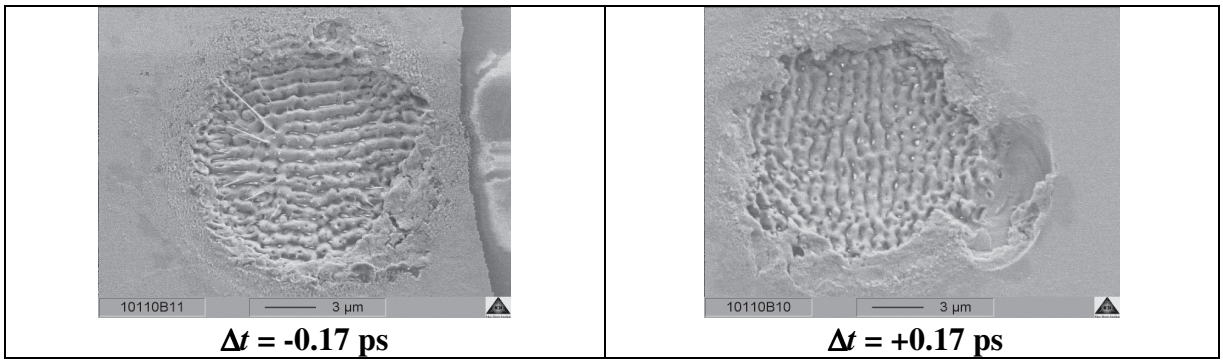

Fig. 1: SEM images of Fused Silica surfaces after irradiation by five cross-polarized double-fs-laser pulses (N_{DPS} = 5, ϕ_{tot} = 7.1 J/cm^2- both pulses together) of two different sub-ps-delays Δt.

Fig. 1 shows an example of LIPSS formation on the surface of the dielectrics material Fused Silica after irradiation by five cross-polarized double-fs-pulses (N_{DPS} = 5, ϕ_{tot} = 7.1 J/cm^2) at two different delay values. The results indicate that the first fs-laser pulse of the pair determines the orientation of the LIPSS (parallel to its laser beam polarization).

Abstracts of Talks

Focus Session „LASER-INDUCED NANOSTRUCTURES“

1. Nanostructure formation at metal surfaces
2. General aspects and structuring in three dimensions
3. Nanostructure formation in semiconductors and dielectrics

Focus Session „NONLINEAR NANOOPTICS“

4. **Plasmonics, metamaterials and nonlinear optics**
5. Spectroscopy, gain materials and characterization

COUPLING SURFACE PLASMON POLARITONS TO EXCITONS IN METAL-J-AGGREGATE HYBRID NANOSTRUCUTRES

P. Vasa,[1,*] R. Pomraenke,[1] W. Wang,[1] M. Lammers,[1] M. Maiuri,[2] C. Manzoni,[2] G. Cerullo,[2] and C. Lienau[1]

[1] Insitut für Physik, Carl von Ossietzky Universität, 26129 Oldenburg, Germany, [2] Center for Ultrafast Science and Biomedical Optics, Dipartimento di Fisica, Politecnico di Milano, Milano, Italy

The optical properties of hybrid nanostructures comprising active materials, e.g., semiconductors or J-aggregated molecules and metals are currently attracting substantial attention since they may form the basis for novel optoelectronic devices.[1] Such nanostructures are fundamentally interesting because, in favorable geometries, the near-field electromagnetic coupling between excitons and surface plasmon polaritons (SPPs) is so strong that their optical response is governed by a new class of short-lived quasiparticles, exciton – surface plasmon polaritons [2], with hitherto essentially unexplored nonequilibrium dynamics. Their binding energies, $E_b = \int \vec{\mu}_{ex}(\vec{r})\vec{E}_{SPP}(\vec{r})d\vec{r}$, given by the overlap of the excitonic transition dipole moment $\vec{\mu}_{ex}$ and the SPP field $\vec{E}_{SPP}$, can reach several hundred meV, allowing for an ultrafast coherent control of their optical properties by externally manipulating either $\vec{\mu}_{ex}$ or $\vec{E}_{SPP}$.

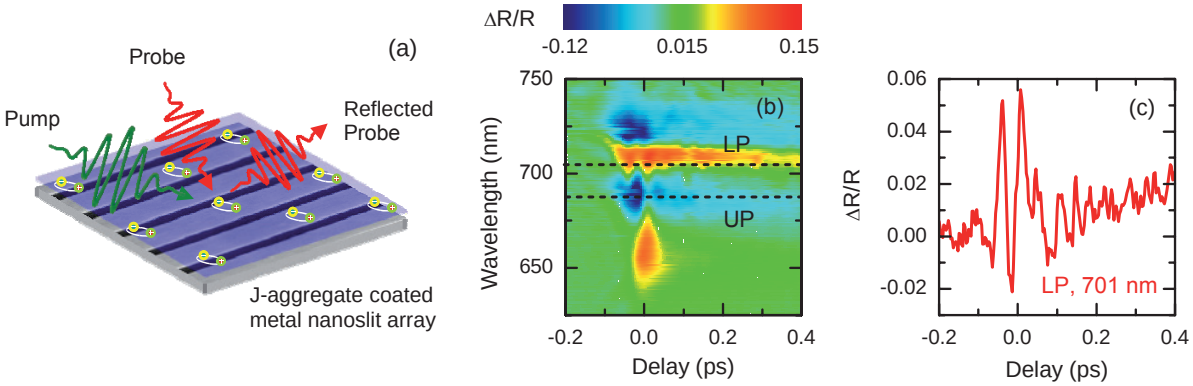

Fig. 1(a) Schematic of the pump-probe experiment performed on a J-aggregate-coated metal nano-slit array, (b) Time-resolved differential reflectivity (ΔR/R) spectra of such a nanostructure recorded at an incidence angle of 30°. The upper (UP) and lower (LP) polaritons resulting from the strong near-field electromagnetic coupling between excitons and SPPs are clearly visible. In the time domain, this coupling gives rise to pronounced, extremely fast coherent Rabi oscillations on the UP and LP resonances as seen in (c).

Here, we study the ultrafast coherent dynamics of exciton-surface plasmon polaritons excitations in metal-semiconductor hybrid nanostructures. A 50-nm-thick J-aggregated cyanine dye film deposited onto a gold grating, displaying strong exciton-SPP coupling with E_b > 50 meV is chosen [Fig. 1(a)]. The ultrafast nonlinear optical response of these nanostructures is studied by recording angle as well as time resolved differential reflectivity spectra [Fig. 1(b)] using a sub-15 fs time resolution pump-probe setup. We demonstrate ultrafast, completely external and fully reversible control over E_b [Fig. 1(b)] by non-resonant optical pumping [2]. When resonantly exciting the nanostructure, we observe, for the first time to our knowledge, pronounced temporal oscillations in the nonlinear optical response [Fig. 1(b,c)] near the polariton resonance wavelengths. These oscillations with a period of ~50 fs are the time-domain signature of Rabi oscillations between excitons and SPP induced by vacuum fluctuations of the electromagnetic near field. When resonantly exciting LP polaritons only, we find, even more interestingly, new, short-lived resonances in the nonlinear optical spectra, clearly reflecting the higher order states of the exciton-SPP Jaynes-Cummings ladder. These resonances are a first direct signature of the quantization of the SPP fields, opening up a new possibility for exploring what may be termed “plasmon quantum electrodynamics”

[1] R. F. Oulton et al, Nature, 461 (2009), pp. 629-632.
[2] P. Vasa et al, *ACS Nano*, 4 (2010), pp. 7559-7565.

*corresponding author : parinda.vasa@uni-oldenburg.de

Direct Laser Writing of Gain and Metallic Nanostructures

Ioanna Sakellari, Elmina A. Kabouraki, Vytautas Purlys, Arune Gaidukeviciute, David Gray, Costas Fotakis, Maria Vamvakaki and Maria Farsari*

Institute of Electronic Structure and Laser (IESL), Foundation for Research and Technology Hellas (FORTH), N. Plastira 100, 70013, Heraklion, Crete, Greece.

*mfarsari@iesl.forth.gr

We present our investigations on the fabrication of three-dimensional nanostructures by direct laser writing using organic-inorganic hybrid materials that (i) can be structured accurately to sub-100nm, (ii) contain quantum dots, and (iii) can be selectively covered with metal.

Direct laser writing by multi-photon polymerization is a nonlinear optical technique which allows the fabrication of three-dimensional structures with a resolution beyond the diffraction limit [1]. The polymerization process is initiated when the beam of an ultra-fast infrared laser is tightly focused into the volume of a transparent, photosensitive material. Multiphoton absorption takes place within the focal volume, where polymerization occurs; by moving the focused laser beam in a three-dimensional manner within the resin, 3D structures can be fabricated. The technique has been employed successfully in the fabrication of nano-photonic structures and devices.

Here, we present our most recent work on the structuring of a series of hybrid organic-inorganic materials by direct laser writing. These materials fall into the following categories:

(i) Hybrid materials containing a quencher, allowing the fabrication of excellent quality photonic crystal woodpile structures with period as low as 500 nm and higher order stop-gaps in visible wavelengths (Figure 1).

(ii) Silicon oxide-based hybrid materials in which quantum dots have been chemically incorporated, enabling gain and the dynamic tuning of the optical properties of the fabricated structures.

(iii) Composite materials with metal binding affinity. These materials can be structured accurately and, due to the incorporated metal binding groups, can be readily metalized with silver and other metals by simple immersion in a metal bath, without the need to modify the surface of the structures or to use other, complementary techniques

The combination of direct laser writing with specially designed, functional materials can lead to advanced applications in photonics, metamaterials and biomedicine.

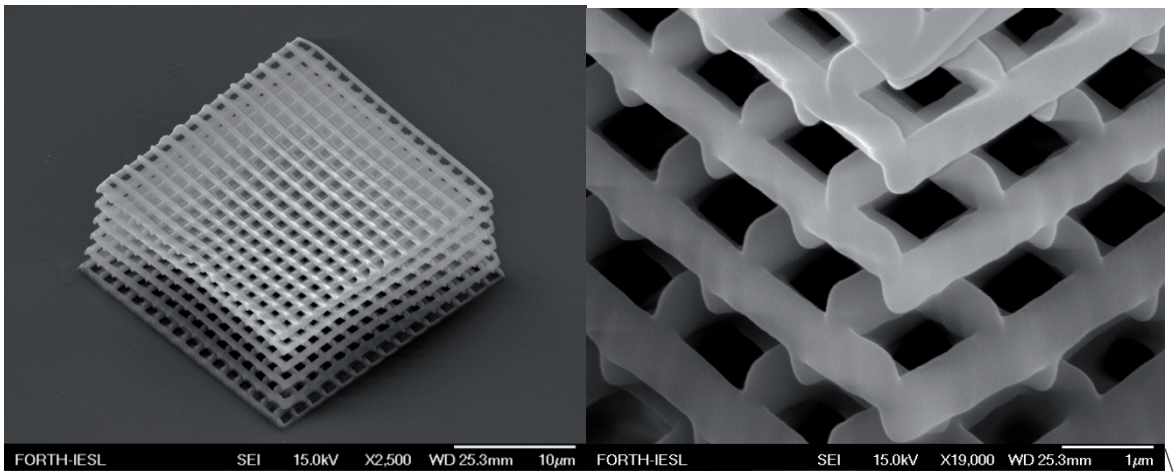

Figure 1: A woodpile structures fabricated using hybrid materials.

References

[1] Sun, H.-B. & Kawata, S. Two-Photon Photopolymerization and 3D Lithographic Microfabrication in *NMR. 3D analysis. Photopolymerization* (ed. N. Fatkullin) 169-273 (Springer Berlin / Heidelberg, 2004).

Towards unraveling the mechanism of third harmonic generation in plasmonic nanoantennas

Mario Hentschel[1,2], Tobias Utikal[1,2], Markus Lippitz[1,2], and Harald Giessen[1]

[1]*4th Physics Institute and Research Center SCoPE, University of Stuttgart, D-70569 Stuttgart, Germany*
[2]*Max-Planck-Institute for Solid State Research, Heisenbergstr. 1, D-70569 Stuttgart, Germany*
m.hentschel@physik.uni-stuttgart.de

Recently, the field of optical nanoantennas has attracted considerable interest. Linear as well as nonlinear optical properties have been the subject of intense investigation. Up to now the nonlinear processes are not well understood.

In this contribution, we aim at unravelling these nonlinear optical properties. Therefore, we investigate third harmonic generation (THG) from a large varied parameter set of optical nanoantenna arrays in order to elucidate the nonlinear efficiency as well as the enhancement mechanism. We fabricated 9x11 arrays of 125x200 nanoantennas each, varying continuously the gap size as well as the bowtie size. Both structural parameters determine the resonance wavelength of these plasmonic dimers, leading to a wide range of resonance positions from 690 nm to 1020 nm. The linear transmittance spectra were measured by a Fourier transform infrared spectrometer (see Fig. 1).

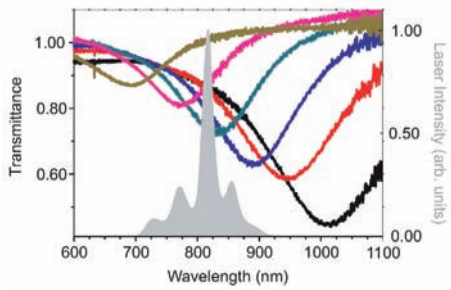

Figure 1: Exemplary linear transmittance spectra of a set of bowtie nanoantenna arrays, showing the wavelength range covered by the plasmon resonance of the structures under investigation. Grey: spectrum of the 8 fs laser source.

8 fs broadband laser pulses with a center wavelength of 820 nm were utilized to generate the third harmonic signal (see Figure 1). For spectrally resolved detection of the THG signal a combined system of a CCD camera and a monochromator was used.

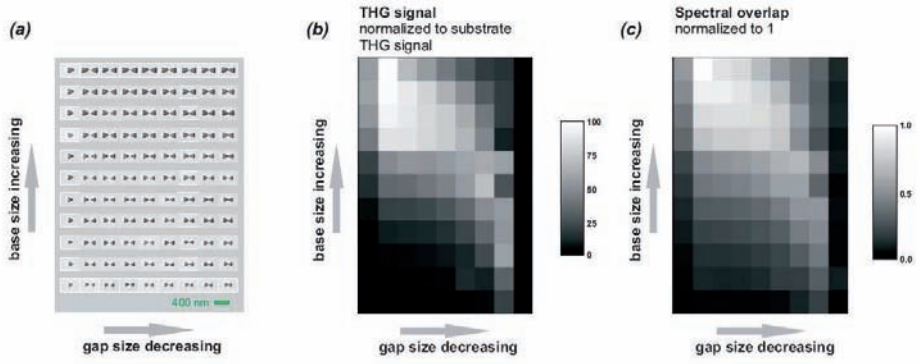

Figure 2: (a) Overview of the bowtie sample design. For each of the 99 bowtie arrays one exemplary antenna is shown. Horizontally the gap size is decreased from half antennas to ohmic contact (smallest gap ~20 nm), vertically the triangle base size is successively increased from ~100 nm to ~200 nm. (b) Integrated THG signal (normalized to the THG signal generated by the bare substrate). (c) Spectral overlap, defined as the sum of the product of the linear extinction spectrum and the spectrum of the broadband laser pulses.

We find that surprisingly the third harmonic signal does not scale with shrinking gap size as expected, but is rather a function of resonance energies in the hybridized plasmonic dimer as well as the plasmonic oscillator strength. The third harmonic signal is strongest for maximum overlap of the extinction spectrum of the nanostructures and the laser spectrum. For a bowtie antenna with base size of ~200 nm the THG signal is strongest for a gap size of ~70 nm and decreases with decreasing gap size as the plasmon resonance is red-shifted due to stronger near-field coupling, hence the overlap of the laser and extinction spectrum is diminishing (see Fig. 2c).

Strong field photoemission from metal nanotips

R. Bormann,[1] M. Gulde,[1] S. V. Yalunin,[1] A. Weismann,[1] and C. Ropers[1,*]

[1] *Courant Research Center Nano-Spectroscopy and X-Ray Imaging, University of Göttingen, 37077 Göttingen, Germany*

Strong-field photoemission at the apex of nanometric gold tips is experimentally and theoretically investigated. The transition between the multiphoton and optical field emission regimes is clearly resolved and theoretically described. The study demonstrates the possibility to observe high-order effects in nanostructures under non-destructive conditions.

Single- and multiphoton photoelectron emission spectroscopy from solids are powerful tools to map electronic band structures [1]. In the study of nanostructures, linear and low order nonlinear interactions of light with metal surfaces have found numerous applications, for example in the form of imaging the spatio-temporal dynamics of surface plasmon excitations by two-photon photoemission microscopy [2]. The study of optical strong-field effects at surfaces – where "strong" refers to the dominance of the light's over the binding fields – is still in its infancy, especially compared with its counterpart in atomic and molecular gases, since the close-by optical damage thresholds and (in the case of photoemission) space charge effects at high carrier densities have rendered such observations much less accessible. Here, we present recent data on strong-field photoemission from single conical nanotips.

Ultrafast electron sources of great spatial coherence combine optical field enhancements at metal nanotips with nonlinear photoelectric effects [4, 5]. In these sources, photoemission from the tip apex is induced using photon energies far below the material's work function. All of the previous experiments in this research field have so far been consistent with a description in terms of (low-order) multiphoton photoelectron emission.

In the present work, we find a transition to the strong-field regime by controllably increasing the peak intensity at these single nanostructures to unprecedented (but non-destructive) values with low repetition rate femtosecond light pulses (central wavelength 800 nm, pulse duration 30 fs, repetition rate 1 kHz) [3].

Figure 1c shows a schematic of the experimental configuration. Light pulses are focused on the tip apex, and the emitted electrons are recorded with a microchannel plate and phosphor screen assembly. The arrival positions on the detector also yield information on the electron emission direction. The experimentally found dependencies on the incident pulse energy demonstrate multiphoton scaling at low intensities and a transition to the tunneling regime near a Keldysh parameter of unity [3], evidencing by reductions of both the effective nonlinearity and the solid angle of the electron emission [cf. Figs. 1a, b]. The deviation from multiphoton behavior is consistent with a theoretical treatment in the strong-field approximation [solid line in Fig. 1a], and the emission cone reduction

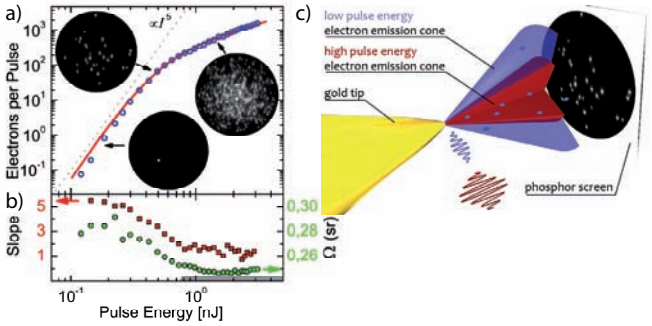

FIG. 1: a) Pulse energy dependence of electron current, showing deviation from pure multiphoton behavior. Blue circles: Experimental data. Red line: Simulation based on strong-field approximation. Insets show exemplary single-shot emission patterns on a phosphor screen detector. b) Pulse energy dependence of effective nonlinearity (red, left axis) and solid angle of the emission cone (green, right axis) [3]. c) Schematic of photoelectron emission from nanometric gold tips.

at high intensities demonstrates a light-induced transfer of forward momentum to the electrons [Fig. 1b]. Measurements of the kinetic energies of the emitted electrons (presented in the talk) support these assertions.

In summary, results on highly nonlinear photoemission and were shown for gold nanotips. It is expected that further studies in this direction will result in increased interest and expansions of strong-field interactions into the domain of nanostructures and interfaces.

We gratefully acknowledge financial support by the Deutsche Forschungsgemeinschaft (DFG-ZUK 45/1 and SPP 1391) and EU Erasmus Mundus.

* Electronic address: cropers@gwdg.de

[1] S. Hüfner, *Photoelectron Spectroscopy: Principles and Applications*, Springer, Berlin (2003).
[2] A. Kubo, K. Onda, H. Petek, Z. Sun, Y. S. Jung, H. K. Kim, Nano Lett. **5**, 1123 (2005).
[3] R. Bormann *et al.*, Phys. Rev. Lett. **105**, 147601 (2010).
[4] C. Ropers *et al.*, Phys. Rev. Lett. **98**, 043907 (2007).
[5] P. Hommelhoff *et al.*, Phys. Rev. Lett. **96**, 077401 (2006).
[6] P. B. Corkum and F. Krausz, Nature Phys. **3**, 381 (2007).

Theory of low-threshold high-order harmonic generation by using field enhancement near metallic fractal surfaces

K.-H. Kim, A. Husakou, J. Herrmann
Max Born Institute, Max Born Str. 2A, D-12489 Berlin

High-order harmonic generation (HHG) [1] is of great importance in modern physics as a valuable tool for attosecond physics, spectroscopy, and others. For high-order harmonics sources at MHz repetition rates, plasmonic field enhancement by nanostructures can be applied [2], requiring however nanolithographic equipment. As an alternative, we consider here rough surfaces which were shown to provide a significant field enhancement in the so-called "hot spots", used e. g. in surface-enhanced Raman spectroscopy.

In this work, we study HHG on the metallic rough surface surrounded by 1-atm argon. The rough surface structure is described by the restricted solid-on-solid model [3] with 1 nm step, which provides a typical self-affine fractal structure commonly obtained during silver deposition. By using the discrete dipole approximation, we determine the frequency-dependent field enhancement distribution and use it to calculate the enhanced pulse intensity in the "hot spots" on the surface, assuming 10-fs, 100-GW/cm^2 of normally incident pump pulses. The structure of generated surface and enhanced field distribution are shown in Fig. 1(a). Localized field enhancement inherent in the fractal surfaces is evident from the figure. The intensity enhancement factor reaches values up to 3000 for a wide spectral range covering the spectral width of few cycle pulses with the central wavelength at 800 nm. Finally, we simulate the HHG by using Lewenstein model [4] averaging over an ensemble of rough surface realizations. We predict the efficiencies of HHG for plateau and cut-off components [see Fig. 1(b)] of 10^{-8} – 10^{-9} which is higher by 1 order of magnitude than the efficiencies obtained for the periodical bow-tie shaped nanostructures [2].

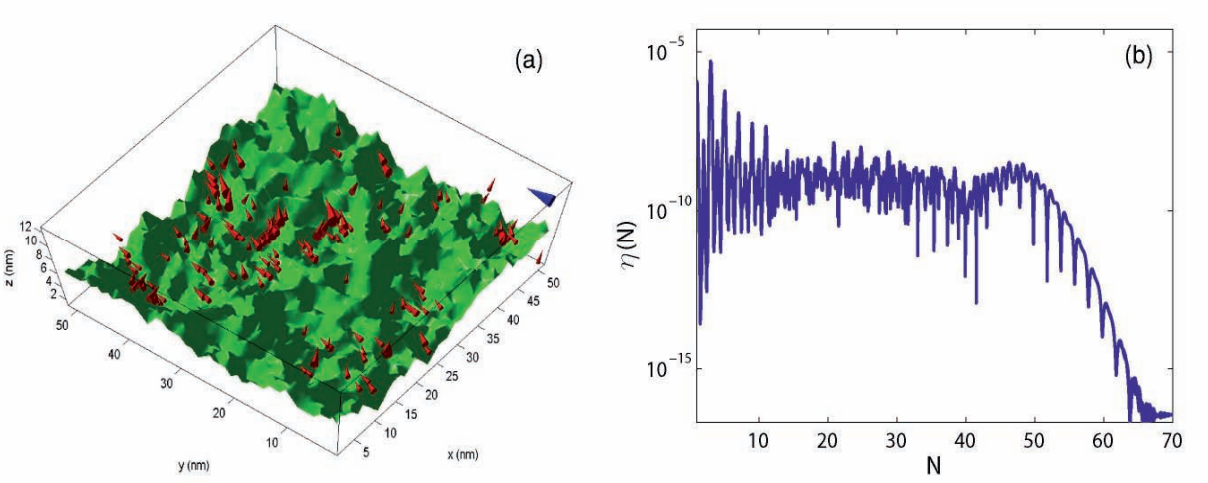

Fig. 1. Generated rough surface and enhanced field distribution (a) and averaged harmonic generation efficiency (b). In (a), red cones show field intensity and its polarization in "hot spots" and blue one shows the direction of incident field polarization.

References

1. F. Krausz and M. Ivanov, Rev. Mod. Phys. **81**, 163 (2009).
2. S. Kim *et al.*, Nature **453**, 757 (2008).
3. V. M. Shalaev *et al.*, Phys. Rev. B **54**, 8235 (1996).
4. M. Lewenstein *et al.*, Phys. Rev. A **49**, 2117 (1994).

Optical Harmonic Generation in Bow Tie Nanoantennas

M. Sivis,[1] M. Duwe,[1] K. R. Siefermann,[2] Y. Liu,[2] B. Abel,[2,3] and C. Ropers[1,*]

[1] *Courant Research Center Nano-Spectroscopy and X-Ray Imaging, University of Göttingen, 37077 Göttingen, Germany*
[2] *Department of Physical Chemistry I, University of Göttingen, 37077 Göttingen, Germany*
[3] *Faculty for Chemistry and Mineralogy, University of Leipzig, 04103 Leipzig, Germany*

Experimental results for resonance enhanced harmonic generation from plasmonic bow-tie nanostructures in the presence and absence of a noble gas jet are presented. Arrays of such nanostructures were exposed to low-energy, few femtosecond light pulses, and harmonic generation in the vacuum ultraviolet is spectrally analyzed.

Plasmonic resonances in nanostructures offer great possibilities for tailoring and controlling local optical fields. The enhanced near-fields in such structures can be used for many linear and nonlinear optical processes, including surface enhanced Raman scattering, second and third harmonic generation or multiphoton photoemission. With few exceptions, such processes involve mostly low-order nonlinearities. Recently, also strong-field effects at plasmonic nanostructures were observed in the form of strong-field photoemission [1] or high harmonic generation [2]. In the latter study, harmonics from the 7^{th} to the 17^{th} order were generated in resonant bow tie nanostructures, demonstrating a possibility for the greatly simplified generation of coherent extreme ultraviolet pulses [2–4]. Despite the great interest in the effect and its mechanism, subsequent experimental reports on this topic and more detailed investigations have not yet been reported, and numerous questions concerning the underlying physics need to be resolved. In particular, the role of the plasmonic resonance on the harmonic spectra, contributions from the gas and intrinsic nanostructure nonlinearities, as well as the scalability of the process have not yet been elucidated.

In this contribution, we follow the approach of Kim *et al.* [2], using the field enhancement in the gap of bow-tie nanostructures to boost harmonic generation for low power incident light pulses. Our structures are fabricated by focused ion beam etching [cf. Fig. 1a] and display both gaps and radii of curvature on the order of 30 nm. The experimental setup is shown in Fig. 2b. It consists of a Ti:sapphire laser oscillator, a harmonic generation vacuum chamber and an EUV spectrometer. Figure 1c shows the observed harmonic emission from bow-tie structures with and without the presence of an Argon gas jet. Interestingly, we find substantial fifth harmonic generation from the bare structures, which has not been reported before. If the gas jet is placed on the structure, this fifth harmonic is only moderately amplified, while a strong seventh order harmonic appears. The relative intensities of different harmonics allow for a determination of the structure-induced intensity enhancement, yielding a value of 250. We expect to achieve higher harmonics by improving nanostructure fabrication conditions.

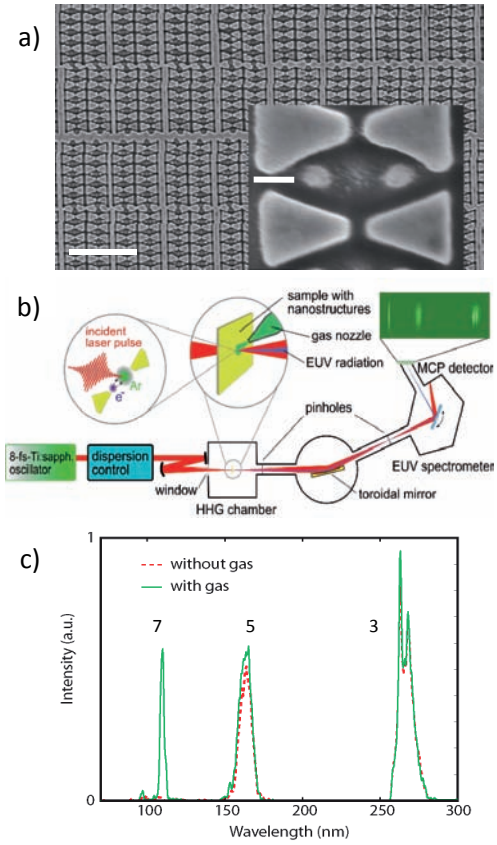

FIG. 1: a) Scanning electron micrograph of bow-tie nanostructure array. Inset: Zoomed-in image of single structures. Scale bars in picture and inset are 2 μm and 100 nm, respectively. b) Experimental setup for the detection of harmonic generation from nanostructures. c) Experimental spectra recorded in the absence (dashed red) and presence (solid green) of an Argon gas jet on the nanostructures, demonstrating third, fifth and seventh harmonic emission.

* Electronic address: cropers@gwdg.de

[1] R. Bormann *et al.*, Phys. Rev. Lett. **105**, 147601 (2010).
[2] S. Kim *et al.*, Nature **453**, 757 (2008).
[3] M. Stockman, Nature, **453** 731 (2008).
[4] A. Husakou *et al.*, arXiv:1009.4124v1 (2010).

Weak localization of light in ZnO nanorods in space and time

M. Mascheck, S. Schmidt, M. Silies, C. Lienau
Institut für Physik, University of Oldenburg, 26129 Oldenburg, Germany

D. Leipold, E. Runge
Institut für Physik, Technische Universität Ilmenau, 98684 Ilmenau, Germany

T. Yatsui, K. Kitamura, M. Ohtsu
School of Engineering, University of Tokyo, 113-8656 Tokyo, Japan

The localization of light in randomly disordered media due to multiple coherent scattering is of high current interest [1,2], since it offers the possibility to locally enhance the interaction with the medium. In nano-optics, surface plasmon polariton localization in metallic nanostructures is known to result in field confinement on a 10 nm scale, enhancement factors of two orders of magnitude and lifetimes of localized plasmon modes extending to several tens of femtoseconds [3], This is readily applied, e.g., in surface-enhanced Raman spectroscopy. Similar field localization effects also occur in random dielectrics, yet are much more challenging to resolve since the corresponding enhancement factors are much smaller. Therefore, they have mostly been investigated using ndirect tools, e.g., coherent backscattering [1]. Here, we visualize, for the first time the weak localization of a light in a randomly arranged array of densely packed ZnO nanorods in both space and time.

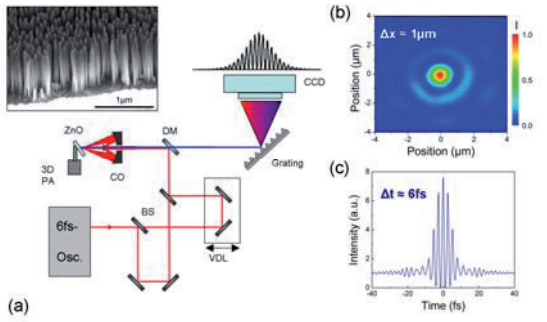

Fig. 2: (a) ZnO nanoneedle array and ultrafast second-harmonic microscope using a pair of 6-fs laser pulses in a dispersion-balanced set-up. (b) Spatial intensity profile of the diffraction-limited few-cycle pulses in the focus of the Cassegrain objective. (c) Interferometric auto-correlation trace recorded in the focal plane of the objective.

Ultrashort laser pulses from a Ti:Sapphire oscillator with a pulse duration of 6 fs are focused to their diffraction-limit of 1 µm^2 onto the ZnO nanorod array using an all-reflective Cassegrain objective (Fig. 1). The generated second harmonic (SH) emission is collected in reflection geometry. Pronounced spatial intensity fluctuations on a sub-µm scale are taken as the spatial signature of the weak loclalization of the fundamental laser light with the dielectric nanoresonators. In Fig. 2, these SH intensity fluctuations are displayed on 40 x 40 µm^2 scale, indicating enhancement factors of more than 80.

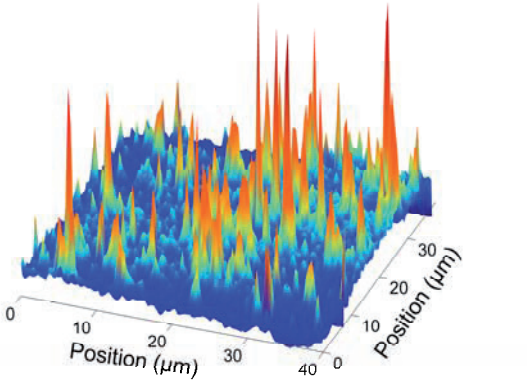

Fig. 2: Spatially-resolved SH emission from the ZnO nanoneedle array after illumination with 6-fs laser pulses centered at 800 nm. We find random SH enhancement by more than a factor of 80 localized to a 500 nm spot size.

By exciting the sample with a phase-stabilized pair of laser pulses from a dispersion-balanced Michelson interferometer and recording SH spectra as function of pulse delay, interferometric frequency-resolved autocorrelation (IFRAC) traces are measured. An analysis of these traces allows to directly retrieve the time structure of the localized electric fields. Field lifetimes of individual hot spots varying between 5 and 15 fs are deduced. To our knowledge this is the first time that such extremely fast localization phenomena in random dielectrics could be resolved in real space and time.

[1] D.S. Wiersma, P. Bartolini, A. Lagendijk, and R. Righini, *Nature* **390**, 671 (1997).
[2] C. Conti and A. Fratalocci, *Nature Physics*, **4**, 794 (2008).
[3] M. I. Stockman, *Phys. Rev. Lett.* **84**,1011 (2000).

Finite-Element Method Simulations of Plasmonic Devices and Materials

Sven Burger
Zuse Institute Berlin (ZIB), Takustraße 7, 14195 Berlin, Germany
JCMwave GmbH, Bolivarallee 22, 14050 Berlin, Germany

Maxwell's equations in combination with specific material properties (realized, e.g., by a combination of a highly-conducting metal like silver and dielectrica) allow for time-harmonic wave solutions which decay exponentially in one or several space dimensions (e.g., surface plasmon resonances). Plasmons can concentrate light in small volumes, far beyond the diffraction limit. At the same time, the spectral response of plasmon resonances critically depends on geometrical and material properties of the experimental arrangement. This allows for a broad variety of interesting applications.

For understanding and designing properties of plasmonic resonators numerical simulations of Maxwell's equations are very helpful. However, rigorous simulations of such setups are challenging because (i) structures and field distributions are defined on multi-scale geometries (e.g., nanometer layers extending over microns), (ii) material properties (e.g., permittivity of silver) lead to high field enhancements or singularities at edges and corners of the objects, (iii) typical regions of interest are 3D and large in scales of cubic wavelengths, (iv) structures often are embedded into inhomogeneous exterior domains (e.g., plasmonic particles embedded into the material stack of a solar cell).

For approaching plasmonic simulation tasks we use dedicated finite-element methods (FEM) developed at JCMwave and ZIB [1]. In this contribution we discuss simulations of several plasmonic devices and effects, ranging from plasmonic nanoantennas for biomolecule detection [2] to helix metamaterial as ultra-thin circular polarizer [3], coupled plasmonic nanoantennas for near-field enhancement [4], hybrid plasmonic waveguide setups for plasmon lasers [5], nanoapertures for extreme transmission enhancement [6] and frequency shifts of resonances in gold microspheres for optical microscopy at sub-wavelength resolution [7].

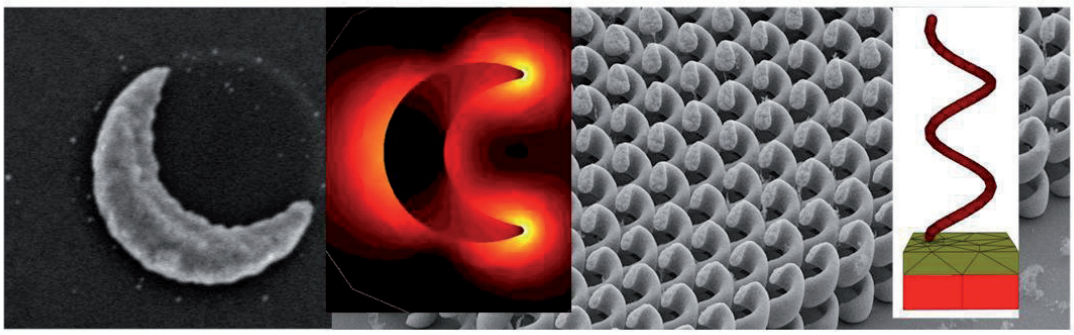

Fig. 1 From left to right: Micrograph of a plasmonic plasmonic nanoantenna [2] (by courtesy of A. Unger, MPIP), intensity distribution of a higher-order resonance, micrograph of an array of nano-helices [3] (by courtesy of J. Gansel, KIT), FEM mesh.

References

[1] S. Burger, L. Zschiedrich, J. Pomplun und F. Schmidt, „JCMsuite: An adaptive FEM solver for precise simulations in nano-optics," Integrated Photonics and Nanophotonics Research and Applications, Optical Society of America, ITuE4 (2008).
[2] A. Unger, U. Rietzler, R. Berger, M. Kreiter, „Sensitivity of Crescent-Shaped Metal Nanoparticles to Attachment of Dielectric Colloids," Nano Lett. **9,** 2311 (2009).
[3] J. K. Gansel, M. Wegener, S. Burger, and S. Linden, „Gold helix photonic metamaterials: A numerical parameter study," Opt. Express **18**, 1059 (2010).
[4] J. Hoffmann, C. Hafner, P. Leidenberger, J. Hesselbarth, S. Burger, „Comparison of electromagnetic field solvers for the 3D analysis of plasmonic nano antennas," Proc. SPIE Vol. **7390**, 73900J (2009).
[5] S. Burger, L. Zschiedrich, and F. Schmidt, „FEM Simulation of Plasmon Laser Resonances," AIP Conf. Proc. **1281**, 1613 (2010).
[6] D. Lockau, L. Zschiedrich, S. Burger, „Accurate simulation of light transmission through subwavelength apertures in metal films," J. Opt. A: Pure Appl. Opt. **11**, 114013 (2009).
[7] T. Kalkbrenner, U. Hakanson, A. Schädle, S. Burger, C. Henkel, and V. Sandoghdar, „Optical microscopy using the spectral modifications of a nano-antenna," Phys. Rev. Lett., **95**, 200801 (2005).

Broadband (~1000 nm) carbon nanotube saturable absorber mode-locking of bulk solid-state lasers

A. Schmidt[1], G. Steinmeyer[1], V. Petrov[1], U. Griebner[1], S. Y. Choi[2], W. B. Cho[2], D.-I. Yeom[2], K. Kim[2], and F. Rotermund[2]

[1] *Max Born Institute, Max Born Str. 2A, D-12489 Berlin, Germany*
[2] *Division of Energy Systems Research, Ajou University, Suwon, Korea*

In recent years, carbon nanotubes have been successfully used as ultrafast saturable absorbers for mode-locking of fiber and bulk solid-state lasers in different spectral ranges [1]. While the widespread SESAMs provide spectrally narrowband coverage and require complex manufacturing processes with additional post-treatment to reduce response times, SWCNT-SAs exhibit broadband absorption with large third-order nonlinearities and require relatively simple manufacturing processes. An additional advantage of SWCNT-SAs is that their absorption band is controllable by varying the nanotube diameters and chiralities, and hence, the wavelength coverage can be engineered within a broad spectral range between 1 and 2 µm. To date, most efforts on passive mode-locking with SWCNT-SAs were restricted to fiber lasers because their single-pass gain is much higher than in bulk solid-state lasers and therefore can easily tolerate large non-saturable losses. For SWCNT-SAs applicable to bulk solid-state laser mode-locking, it is mandatory to decrease the losses to the lowest level possible. Most recently, single mode-locking devices providing broad ultrafast saturable absorption and low non-saturable loss were reported by carefully controlling SWCNT bundling and curl in an optimized manufacturing process. This SWCNT-SA was successfully employed for mode-locking of different bulk lasers operating at wavelengths between 1.0 and 1.5 µm [2]. Further progress in the development of such SWCNT-SAs was achieved by mixing two differently grown SWCNTs (Arc-discharge- and HiPCO-made), yielding new SWCNT-SA devices featuring an octave-broad operation bandwidth of about 1000 nm.

The nonlinear response of the SWCNT-SA was measured by pump-probe spectroscopy at different wavelengths in the 1-2 µm range and similar fast bi-exponential behaviour was observed, with the slow component of < 2 ps, corresponding to the interband carrier recombination process in semiconducting SWCNTs. The nonlinear transmission experiments confirmed a low level of non-saturable absorption of ~1.0% together with typical modulation depths of < 0.5% and a saturation fluence of < 10 µJ/cm^2.

For mode-locking over a wide wavelength range based on one and the same SWCNT-SA, we chose four bulk solid-state lasers operating at wavelengths between 1 and 2 µm. Yb:KLuW, Cr:forsterite, Cr:YAG and Tm:KLuW were used as the laser gain materials. The SWCNT-SA mode-locked Yb:KLuW, Cr:forsterite and Cr:YAG lasers at 1.07, 1.25 and 1.49 µm, respectively, generated nearly Fourier-limited pulses with pulse durations of 84-118 fs (assumed sech^2-shaped pulses), whereas the Tm:KLuW laser delivered ~25 ps long pulses at 1.94 µm without dispersion compensation. In all cases, the recorded radio frequency spectra of the fundamental beat note at the laser repetition frequency exhibited extinction ratios with the noise level being > 55 dB below carrier. This is an evidence for stable continuous-wave single-pulse mode-locking without Q-switching instabilities in the operation range between 1 and 2 µm.

References

1. T. Hasan *et al.*, Adv. Mat. **21** (2009) 3874-3899.
2. W. B. Cho *et al.*, Adv. Funct. Mat. **20** (2010) 1937-1943.

Abstracts of Talks

Focus Session „LASER-INDUCED NANOSTRUCTURES“

1. Nanostructure formation at metal surfaces
2. General aspects and structuring in three dimensions
3. Nanostructure formation in semiconductors and dielectrics

Focus Session „NONLINEAR NANOOPTICS“

4. Plasmonics, metamaterials and nonlinear optics
5. **Spectroscopy, gain materials and characterization**

Ultrafast electron transport suppression in Au nanowire networks

E. Magoulakis[1], A. Kostopoulou[1], C. Brintakis[1], A. Andriotis[1], A. G. Kanaras[2], A. Lappas[1] and P. A. Loukakos[1]

[1] Foundation for Research and Technology-Hellas, Institute of Electronic Structure and Laser, N. Plastira 100, P.O. Box 1385, 71110 Heraklion, Greece.
[2] School of Physics and Astronomy, University of Southampton, Southampton, SO17 1BJ, U.K.

A comparative study of the ultrafast dynamics in three dimensional Au nanowire networks (NWN) (Fig. 1) with Au thin films (TF), with thickness equal to the overall diameter of the NWN, following ultrashort laser excitation using time-resolved optical spectroscopy has been carried out. The NWN were prepared by the reduction of the $HAuCl_4 \times 3H_2O$ gold precursor from $NaBH_4$. From the transient absorption (ΔA) traces (Fig. 2), we observe that $|\Delta A|$ reaches its maximum faster in NWN due to the increased electron-electron scattering arising from the volume confinement [1]. Because the relaxation mechanisms depends on temperature, in order to directly compare the relaxation of $\Delta A(t)$ in the two systems we plot the decay times as a function of absorbed energy *per atom* (Fig. 3) to ensure similar excitation conditions. By investigation of the low excitation regime we find similar electron-phonon coupling strength in both systems, while by investigation of the high excitation regime we find that energy transport is suppressed in the Au NWN. We attribute this suppression to the increased number of edges and corners present in the NWN that serve as localization and trapping centres for the excited electrons.

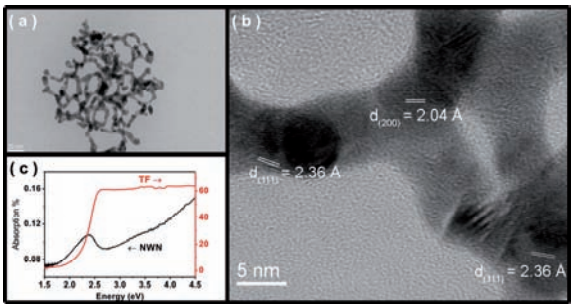

Fig. 1: (a) TEM and (b) high-resolution TEM images of Au NWN. (c) Absorption spectra of Au NWN and TF.

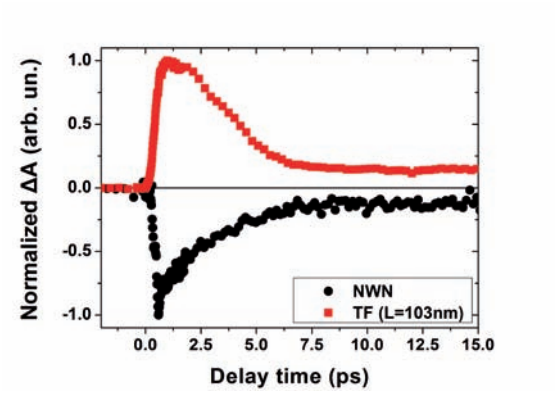

Fig 2: Transient absorption traces of Au NWN and 103 nm thick TF.

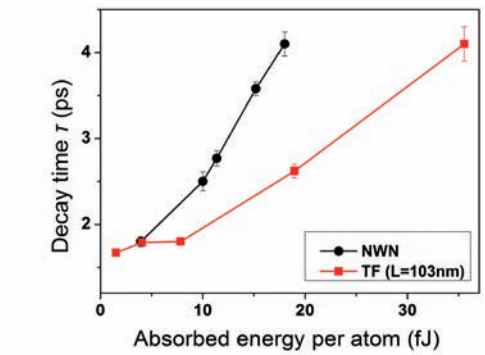

Fig 3: Transient absorption decay times as a function of absorbed energy *per atom* for Au NWN and 103 nm thick TF.

[1] C. Voisin et al., Phys. Rev. B 69, 195416 (2004).

PICOSECOND THG OF ZnO-CONTAINING ORGANIC-INORGANIC NANOCOMPOSITES

I. Kityk

Electrical Engineering Department, Czestochowa University Technology, Armii Krajowej 17, Częstochowa, Poland

The study of the third harmonic generation (THG) for the 40 ps Nd:YAG fundamental laser beam was performed for the different kinds of ZnO-containing organic nanocomposites. The two principal types of ZnO nanocomposites were explored. The ZnO nanocrystallites are embedded into the polymethylmethacrylate (PMMA) and polycarbonte (PC) polymer matrices. The nanocomposites were prepared from the nanocrystallites embedded into the polymer matrices as well as were deposited onto the ZnO NP. Additional experiments were done for the ZnO nanocomposites with additional Au NP. The THG was measured for the ZnO NC sizes varying within the 10 nm – 50 nm range and for different concentration of the ZnO NC determining the inter-particle sizes. It was shown that a substantial increase of the THG with decreasing diameters of the THG appears. However, the effect was stronger for the PC matrices which possess higher polarization with respect to PMMA. Addition of Au NP substantially changes the size and concentration dependence of the third order susceptibilities. Such changes may be explained by additional contribution of the surface plasmon resonances into the third order susceptibilities. The principal role in the observed effects was determined by the interfaces between the polymers and the nanosheet surfaces of the NC. The threshold damage was about 270 mJ/cm^2 for the PMMA nanocomposites and 410 mJ/cm^2 for ZnONC.

Determination of the photoluminescence quantum efficiency of silicon nanocrystals by laser-induced deflection

W. Paa, Ch. Mühlig, K. Potrick, T. Schmidt, S. Bublitz, F. Huisken

We report about the application of a special direct absorption measuring method using laser induced deflection (LID) of a probe beam to determine absorption of thin films with high sensitivity and high precision. After a short introduction to the measurement principle (left figure) and its advantages, we will demonstrate its potential in the case of silicon nanocrystals and other examples.

During oxidation of the freshly grown silicon nanocrystals we use the measurement of the absolute thin film absorption to calculate the photoluminescence quantum efficiency. This allows to track the oxidation process and to observe the ongoing surface oxidation of the nanocrystals until – after a passivation process with a time constant of 8 days – finally a saturation value of the photoluminescence of 65% is reached (right figure). Since for the measurement process the thin film (i.e. the Si nanocrystals) can be regarded a just an absorbing layer it will be also possible to investigate e.g. permanent changes due to defect formation, damage and/ or changes by laser irradiation.

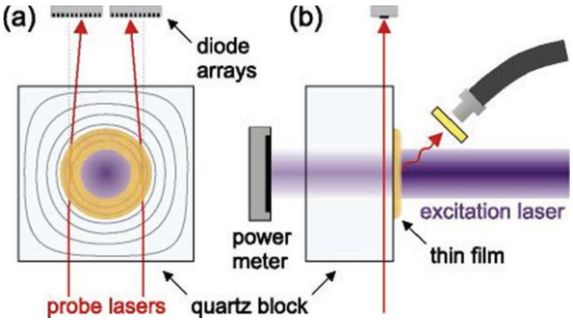

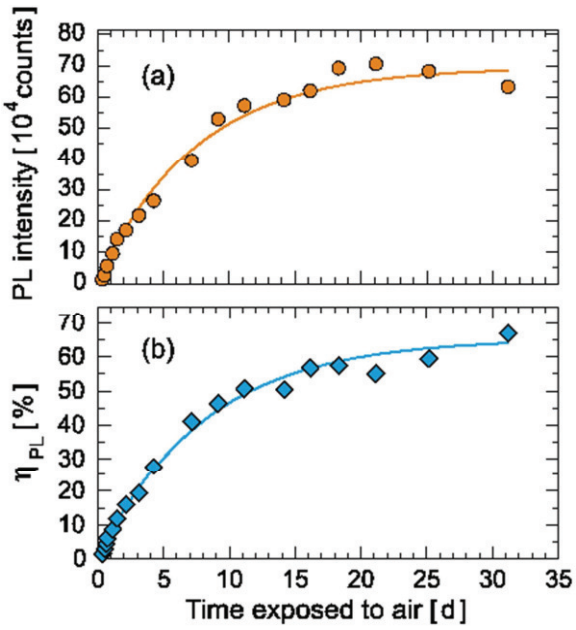

Real-space distribution of cavity modes in single ZnO nanowires

F. Güell,[a*] A. R. Goñi,[b] J. O. Ossó,[c] L. A. Pérez,[d] E. A. Coronado,[d] A. Cornet,[a] J.R. Morante[a,e]

[a] *Departament d'Electrònica, Universitat de Barcelona, E-08028 Barcelona, Catalunya, Spain*
[b] *ICREA Research Prof., ICMAB-CSIC, Campus UAB, E-08193 Bellaterra, Catalunya, Spain*
[c] *MATGAS 2000 A.I.E., Campus UAB, E-08193 Bellaterra, Catalunya, Spain*
[d] *INFIQC, CLCM, Depto. de Fisicoquímica, Facultad de Ciencias Químicas, UNC, Córdoba 5000, Argentina*
[e] *IREC, Institut de Recerca en Energia de Catalunya, E-08930 Sant Adrià de Besòs, Catalunya, Spain*
* Corresponding author: frank@el.ub.edu

Scanning near-field optical microscopy (SNOM) has become nowadays a very powerful technique for investigating the optical properties of nanostructures with a sub-wavelength spatial resolution below 100 nm, such as waveguiding effects in ZnO nanowires (NWs) [1–2]. A spatially resolved study of the electromagnetic field distributions of different cavity modes in ZnO NWs is still lacking. In this work, we have used a near-field optical microscope to map out the evanescent fields of optically excited single-crystal ZnO NWs. The SNOM measurements were performed at room temperature in transmission-collection mode using four different laser wavelengths (378, 514, 633 and 785 nm). They reveal a different spatial distribution of the electromagnetic fields associated to each cavity mode, which are unique properties of the NWs depending primarily on their size and the wavelength of the mode. Figures 1(a) and 1(b) show an example of the SNOM measurements performed on a ZnO NW of approx. 260 nm in diameter at normal incidence from the substrate side, using unpolarized UV (378 nm) and red (633 nm) excitations. The SNOM patterns are quite different. Whereas for UV illumination the pattern exhibits two well defined bright lines running along the edges of the upper hexagonal facet of the wire, for red laser excitation the SNOM pattern displays a strong but wider maximum at the center of the facet. The latter also exhibits a periodic modulation of the near-field intensity all along the axis of the wire. In order to interpret the experimental findings, we have performed electrodynamics simulations using the discrete dipole approximation (DDA), which is an accurate numerical method in which the object of interest is represented as a cubic lattice of N polarizable points [3]. We used about 890000 dipoles to describe the ZnO NW, out of a total of 1.5 million for taking also the substrate into account. Figures 1(c) and 1(d) show the results for the leading modes at the corresponding laser wavelengths. The plots represent the field distribution in cross section of a hexagonal wire supported by a quartz substrate on one of its facets and with true dimensions, as obtained from the topography SNOM profiles. The false color scale corresponds to the field intensity normalized to that of the incident light. We notice the striking qualitative agreement between calculated and measured field distributions.

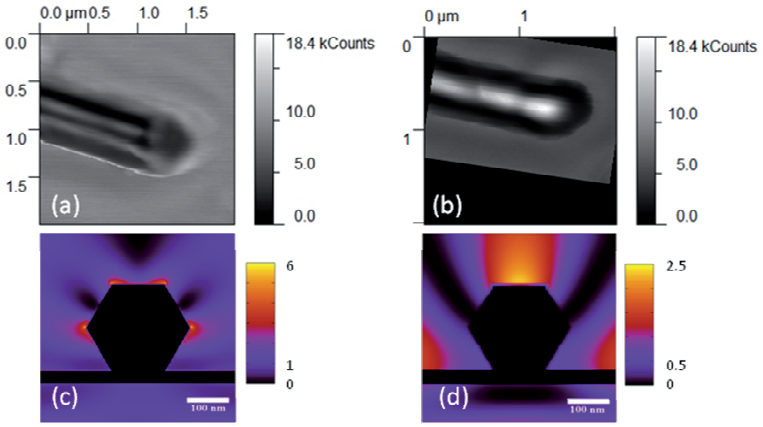

Local Nano-Structure and Morphology of Organic Thin Films

Segei Kühn

Max-Born-Institut für Nichtlineare Optik und Kurzzeitspektroskopie, Max-Born-Str. 2a, 12489 Berlin, Germany

Organic materials are provoking the interest of electro-optical device designers and high performance applications are already conquering the consumer market. But what is more, they constitute a rich field of research for material scientists from different fields. In contrast to their inorganic counterparts, these materials consist of molecules with different degree of complexity offering an enormous potential to tune their specific electronic, chemical and optical properties and thereby their interaction amongst each other and with adjacent building blocks such as supporting materials, and also their reaction to electric fields, chemical agents and light. The causal link from a starting solution over the processing procedure to a desired thin film property is not always evident. Specialized methods are required to obtain a comprehensive understanding.

In this contribution we present a way to determine the local structural quality of a crystalline organic thin film using absorption spectroscopy in parallel with the local morphology using polarization microscopy. Specifically, the material studied consisted of a 100 nm thin film spin-coated from a solution of the size-fractioned dimer of *(P)*QT-12 (alkyl substituted *(poly-)* quaterthiophene [1]). To achieve the spatial resolution on the order of 100 nm, as demanded by the texture of the thin film, we apply near-field optical scanning probe techniques which are perhaps among the least perturbative methods to study such delicate materials. We deduce a film morphology described by an extended quasi-crystalline structure with distributed defects and few hard gain boundaries [2]. The fraction of well crystallized molecules is on the order is generally high, on the order of 80%. This interpretation is supported by data obtained from other techniques such as AFM, TEM and X-ray diffraction and explains the peculiar electronic transport properties of the film [1]. The method offers the possibility of local *in-situ* monitoring of transformations during optical material processing.

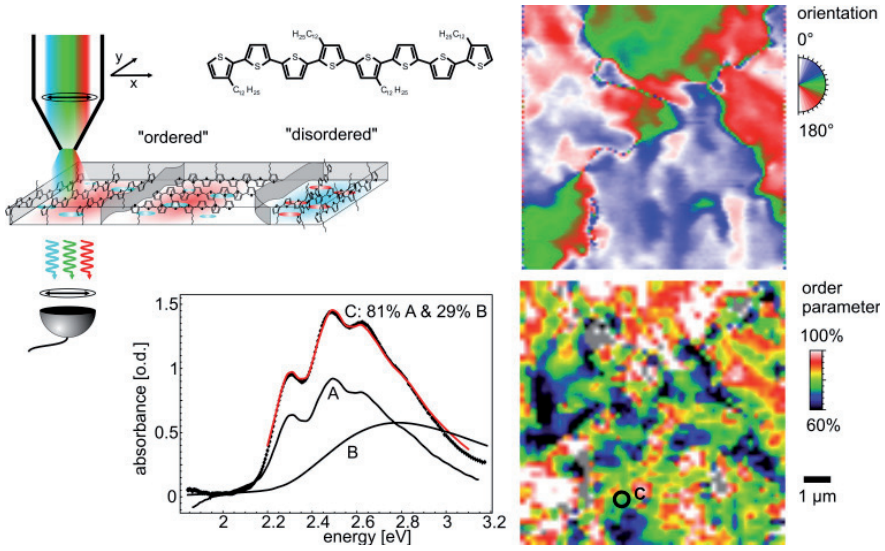

References:
[1] Pingel, P.*et al.*, Applied Physics A: Materials Science & Processing, 2009, 95, 67-72
[2] Kuehn, S.; *et al.*, Adv. Funct. Mater., 2011, 21, 860-868

Abstracts of Posters

Characteristics of ions emitted from the nano-ablation processes with femtosecond laser pulses of the fluence near ablation threshold

Yasuhiro Miyasaka, Masaki Hashida, Yoshinobu Ikuta, Shigeki Tokita, and Shuji Sakabe

Advanced Research Center for Beam Science, Institute for Chemical Research, Kyoto University, Gokasho, Uji, Kyoto 611-0011, Japan and Department of Physics, Graduate School of Science, Kyoto University, Kitashirakawa, Sakyo, Kyoto 606-8502, Japan

By irradiating femtosecond laser pulses on metals at the fluence near the ablation threshold , we detected high energetic ions, of which generation cannot be explained by thermal processes. In the experiments, pulses (λ=800 nm, τ=170 fs, 10 Hz, p-polarized) generated with the T^6 laser system[1] were used. The transverse mode of the pulse is Gaussain. The target was 99.99%-purity Copper metal, of which size was 10×10 mm^2 and the thickness was 1 mm. The target was polished for 1.5-nm roughness of arithmetic mean value and washed in an acetone solution by an ultrasonic cleaning. Figure 1 shows typical Time of Flight (TOF) signals for different laser fluences. The identity of the ion species was confirmed using an energy filter assembled in front of the ion detector. The fast component (t < 30 μs) was protons and the slow component (t >70μs) was Cu ions. The ablation rate is ~0.01nm/pulse at the fluence close to the threshold[2] and only a few ions are emitted. The TOF signals are obtained by accumulating 1500 signals. The TOF signals of Cu ions have peak energy of 22 eV for 40 mJ/cm^2 and 29 eV for 60 mJ/cm^2. The peak energy becomes higher as the fluence increase. To know the characteristics of ion emissions near ablation threshold, angular distribution of ions was also measured. It was found that the ions were emitted to the direction normal to the target surface with high directivity. In this paper, the characteristics (energy spectra and angular distributions) of emitted ions and the emission process are discussed.

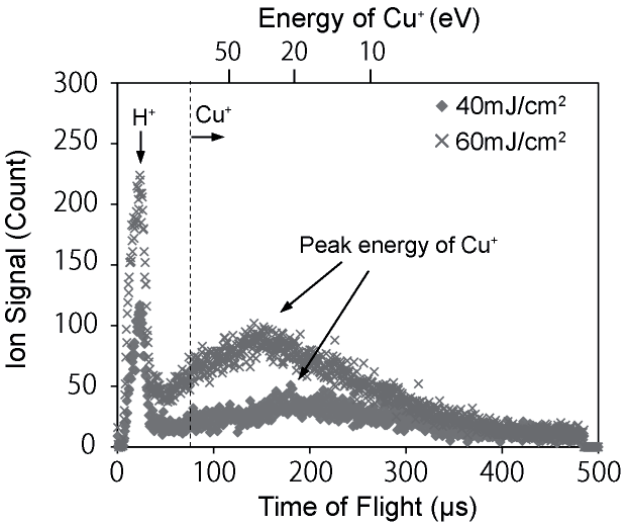

Fig. 1. TOF spectra of ions emitted from Cu surface

[1]S. Tokita et al., Opt. Express **16** (2008) 14875 .
[2]M. Hashida el al. Appl. Surf. Sci. **197-198**(2002)862.

3D Active Photonic Nanostructures

Elmina A. Kabouraki [1,2*], Ioanna Sakellari[1,3], Costas Fotakis[1,3], Maria Vamvakaki[1,2] and Maria Farsari[1]

[1]*Institute of Electronic Structure and Laser (IESL), Foundation for Research and Technology Hellas (FORTH), N. Plastira 100, 70013, Heraklion, Crete, Greece.*

[2] *Department of Materials Science and Technology, University of Crete, Greece.*

[3]*Department of Physics, University of Crete, Greece.*

elmina@iesl.forth.gr

We present our most recent results on the fabrication of 3D high-resolution nanostructures containing Cadmium Sulfide (CdS) quantum dots (QDs) and exhibiting higher order diffraction patterns and stop-gaps at visible wavelengths. These are fabricated using direct laser writing (DLW) and novel, organic-inorganic hybrid materials.

DLW by multi-photon polymerization is a nonlinear optical technique which allows the fabrication of 3D structures with a resolution beyond the diffraction limit [1]. The polymerization process is initiated when the beam of an ultra-fast laser is focused into the volume of a transparent, photosensitive material. Multi-photon absorption takes place within the focal volume, where polymerization occurs. By moving the focused laser beam in a three-dimensional manner within the material, 3D structures can be fabricated.

The materials used in this work are photostucturable organic inorganic hybrid materials prepared using the sol-gel process. This versatile technique has been exploited for the incorporation of inorganic networks into polymer matrices, using as monomers molecules that carry an inorganic part (which serves as the precursor to the inorganic network) and a polymerizable organic group (which acts as the precursor to the organic polymer). In the present work, we have included in the composite a quencher, allowing the fabrication of features well below the diffraction limit, and quantum dot precursors, enabling the *in situ* synthesis of CdS QDs.

We first prepared a composite material based on a polymerizable silicon precursor, and a cadmium-containing organic salt. Next, the inorganic siloxane network was formed by the sol-gel process, whereas, the photosensitivity that this material demonstrates, allowed its 3D laser structuring. Microstructures with spatial resolution below 100 nm and minimal shrinkage distortion were fabricated (Figure 1a). Then, the microstructures were reacted with Na_2S, leading to the *in situ* synthesis of CdS quantum dots within the volume of the 3D structures. The X-Ray diffraction pattern of a CdS containing films showed three broad peaks attributed to the crystalline cubic structure of the nanoparticles. The UV-VIS absorption spectra showed a series of overlapping peaks, which are characteristic of poly-disperse CdS quantum dots formed within the material. Fluorescence spectroscopy was used to measure the emission attributed to the CdS nanoparticles which was found in the visible region of the spectrum. Excellent quality photonic crystal woodpile structures with period as low as 500 nm were fabricated. For the first time in such structures, we show the existence of diffraction patterns and higher order stop-gaps at visible wavelengths (Figures 1b, 1c).

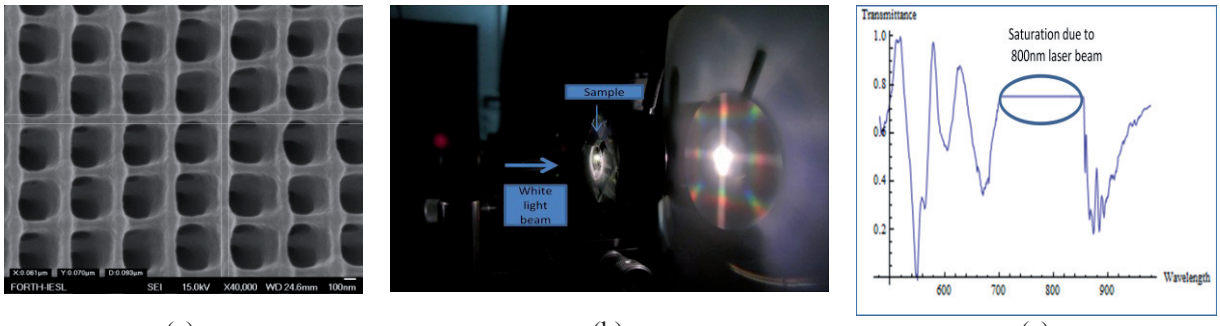

(a) (b) (c)

Figure 1: A woodpile structure (a) fabricated using a hybrid organic-inorganic composite, containing CdS QDs. The high quality and periodicity of the structures is demonstrated by the presence of higher order diffraction patterns and stop-gaps at visible wavelengths (b,c)

References

[1]H.-B. Sun, and S. Kawata, "Two-Photon Photopolymerization and 3D Lithographic Microfabrication " in *NMR. 3D analysis. Photopolymerization* N. Fatkullin, ed. (Springer Berlin / Heidelberg, 2004), pp. 169-273.

Enhanced third order nonlinearity in nanocrystalline TiO_2 thin films

S. K. Das[1], C. Schwanke[1], M. Bock[1], A. Pfuch[2,3], W. Seeber[3], and R. Grunwald[1]

[1]*Max Born Institute for Nonlinear Optics and Short-Pulse Spectroscopy, Max-Born-Strasse 2a, D-12489 Berlin, Germany*
[2]*Friedrich-Schiller-Universität Jena, Otto-Schott-Institut, Fraunhoferstr. 6, D-07743 Jena, Germany*
[3]*INNOVENT e.V., Prüssingstraße 27 B, D-07745 Jena, Germany*

Because of local field enhancement, nanostructured materials can show significantly increased optical nonlinearities compared to bulk material [1]. TiO_2 is a material with particularly high intrinsic third order nonlinear susceptibility. Together with the surface contribution, one can expect extremely high optical conversion efficiencies in nanostructured forms of this material which is of increasing interest for applications like 2D pulse diagnostics. Gayvoronsky et al. [2] reported on third order nonlinearities of $\chi^{(3)}=2\times10^{-5}$ esu which were 6 orders of magnitude above the known values for bulk TiO_2. These results were obtained with 40 ps laser pulses at 1064 nm in a nanoporous TiO_2 (anatase-type) layer. In this study, the effect was determined by measuring the change of the nonlinear refractive index of the material through observating the variation of transmittance. The enhancement was explained by a resonant excitation of electronic defect states at the surface of nanoparticles. In such a long-pulse regime, however, a significant falsifying contribution to the refractive index may come from thermal effects as well which were ignored in the paper. In our case we used the surface third harmonic generation (STHG) method to measure the pure electronic third order optical nonlinearity in the nanostructured thin film of TiO_2. STHG is a phenomena by which one can observe very high third harmonics by focusing the Gaussian beam into the interface of two media with different third order susceptibilities [3]. In the presence of an additional nanolayer, the efficiency of the STHG can further increase. By analysing this signal enhancement, the third order susceptibility can be estimated according to [4] as follows:

$$I(3\omega)_{sub} = HI_{\omega}^{3}\left|\chi_{subs}J(b,\Delta k_{sub})\right|^{2} \quad (1)$$

$$I(3\omega)_{tf} = HI_{\omega}^{3}\left|\chi_{sub}J(b,\Delta k_{sub}) - \chi_{tf}J(b,\Delta k_{tf})\right|^{2} \quad (2)$$

Here, $I(3\omega)_{sub}$ and $I(3\omega)_{tf}$ represent the STHG signal intensities for the pure substrate-air interface and with an additional nanolayer, respectively. Inserting realistic values for the parametric constant H, the phase matching integral $J(b,\Delta k_i)$, third order nonlinearity of the substrate (χ_{sub}) and the ratio of $I(3\omega)_{tf}$ to $I(3\omega)_{sub}$ one can easily derive the third order susceptibility of thin film χ_{tf}. For our case this ratio was found to be around 30:1. and χ_{tf} was calculated to be ~ 2.4 x 10^{-10} esu, a value more than 2 orders of magnitude higher than that for bulk TiO_2. This enhancement is purely due to the surface enhancement and free from any thermal effects. So the nano-material should be capable to work as frequency converter for third order autocorrelators for extremely short pulses at wavelengths around 800 nm.

References:

[1] G. I. Petrov et al., Appl. Phys. Lett. **83**, 3993 (2003).
[2] V. Gayvoronsky et al., Appl. Phys. **B 80**, 97-100 (2005).
[3] T. Y. F. Tsang, Phys. Rev. A **52**, 4116 (1995).
[4] J. M. Schins et al., J. Opt. Soc. Am. **B 19**, 1627 (2002).

Compact and tunable sub-20 fs laser source for ultrafast nonlinear applications

Bernd Metzger,* Andy Steinmann, Gelon Albrecht, and Harald Giessen
4th Physics Institute and Research Center SCoPE, University of Stuttgart, Pfaffenwaldring 57, 70550 Stuttgart, Germany
**Corresponding author: b.metzger@physik.uni-stuttgart.de*

Ultrashort laser pulses pave the way to a variety of new possibilities both in science and in applications. Especially in the discipline of nonlinear optics, the high peak intensities of these new light systems allow to observe effects such as supercontinuum generation already at moderate average power levels. Furthermore the ultrashort time behavior of such pulses enables the investigation of effects also on an ultrashort time scale, for example in semiconductors or plasmonic metamaterials.

To generate ultrashort laser pulses we use ytterbium based solitary mode-locked oscillators, which can be pumped by very inexpensive laser diodes in the near infrared. For the experiments presented here, we use an Yb:KGW oscillator [1], which emits laser pulses at 1025 nm with durations in the range of 200 fs and average powers of several watts at 44 MHz repetition rate.

To obtain smaller pulse durations, we have to increase the bandwidth of our laser pulses. For non-amplified laser systems highly nonlinear optical fibers are perfectly suited for the spectral broadening of laser pulses [2]. In our case tapered fibers are employed [3], since they can be manufactured easily and with great versatility. Therefore the adjustment of different fiber parameters such as the waist diameter and the waist length can be used to optimize the nonlinear propagation in the fibers with respect to the pump laser system.

After spectral broadening, the laser pulses are not transform-limited, due to the dispersion in the fiber. Compression down to 26 fs can be achieved with a simple prism sequence [1]. However, to get closer to the Fourier transform limit, more advanced techniques have to be used. To get rid of arbitrary orders of chirp, we use a grating-based 4-f pulse shaper with a spatial light modulator (SLM) in its Fourier plane. The focal length of the parabolic mirrors in our setup is 444.5 mm, and the SLM consists of 2*640 liquid crystal pixels for phase and amplitude modulation. To find the appropriate phase for the generation of transform-limited pulses we make use of the multiphoton intrapulse interference phase scan (MIIPS) [4]. This method is characterized by fast convergence, since it requires only very few iteration steps.

Fig.1 (left) shows the measured MIIPS trace of the 8th iteration step. Fig.1 (right) depicts the corresponding measured spectrum and autocorrelation of the generated laser pulses. The MIIPS trace as well as the autocorrelation show that the pulses are very close to the transform limit at $\tau_{Pulse} \lesssim 20$ fs.

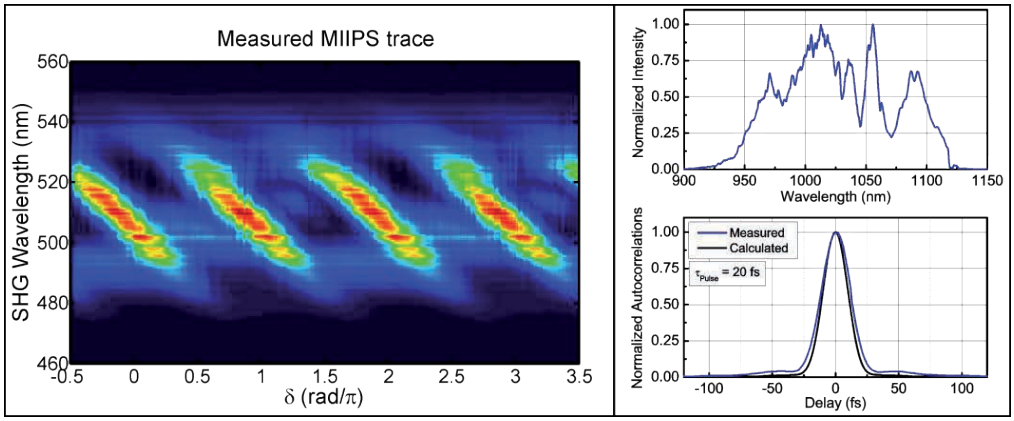

Fig. 1 Left: Measured MIIPS trace of the last iteration step of the MIIPS algorithm. Right: Measured spectrum and measured autocorrelation after the last MIIPS iteration step. The black autocorrelation curve is calculated from the measured spectrum and hence represents the transform limit for the pulses. The average output power is 50 mW.

References

[1] B. Metzger, A. Steinmann, F. Hoos, S. Pricking, and H. Giessen, "Compact laser source for high-power white-light and widely tunable sub 65 fs laser pulses," Opt. Lett. **35,** 3961 (2010).
[2] G. Krauss, S. Lohss, T. Hanke, A. Sell, S. Eggert, R. Huber, and A. Leitenstorfer, "Synthesis of a single cycle of light with compact erbium-doped fibre technology," Nat. Photon. **4,** 33 (2010).
[3] T. A. Birks and Y. W. Li, "The Shape of fiber tapers," J. Lightwave Technol. **10,** 432 (1992).
[4] V. V. Lozovoy, I. Pastirk. and M. Dantus, "Multiphoton intrapulse interference. IV. Ultrashort laser pulse spectral phase characterization and compensation," Opt. Lett. **29,** 775 (2004).

Germanium Nanowire Growth

R. Bansen, J. Schmidtbauer, T. Teubner,
H.P. Schramm and T. Boeck

Abstract

One-dimensional structures such as nanotubes and nanowires were investigated intensively in recent years for various applications. In the field of 3-dimensional nanoelectronics, nanowires have been proposed as promising building blocks for further miniaturized nanodevices. Recently, a renewed interest in germanium for electronic applications arose due to the higher electron mobility and higher intrinsic carrier concentration, compared to silicon and due to the fact that germanium compatible dielectric layers on silicon substrates are now available.

In this poster we focus on the growth of germanium nanowires. They are homoepitaxially obtained by means of the VLS (vapor-liquid-solid) method in a MBE-chamber using effusion cells and electron beam evaporators. Gold droplets are used as metal catalyst. The droplet formation has been investigated depending on substrate temperature and gold evaporation rate.

Growth parameters of the nanowires such as substrate temperature and evaporation rate have been varied to control the growth rate, the diameters and the number of nanowires per unit area. The dependence of nanowire growth on the substrate orientation was investigated systematically by using ⟨100⟩, ⟨110⟩ and ⟨111⟩ oriented germanium substrates.

The prepared samples were characterized by AFM, SEM and TEM studies, which showed epitaxial nanowire growth. Furthermore, our investigations revealed that the wires preferentially grow along the ⟨110⟩, even when ⟨100⟩ and ⟨111⟩ oriented substrates are employed.

Studies of bound exciton and surface excitonic emissions in nanostructured and bulk ZnO

M. Biswas[1], K. Kumar[1], G. Hughes[1], D. McCabe[1], K. Johnston[1], Marc Dietrich[2], E. Alves[3], M. Xia[4], M.O. Henry1, E. McGlynn[1],

[1]School of Physical Sciences and National Centre for Plasma Science and Technology, Dublin City University, Dublin, Ireland.

Research in ZnO has occupied a prominent position in the physics and materials community over the past decade, with attention focussed mainly on the areas of p-type doping and nanostructure growth and characterisation. The microscopic nature of the electronically and optically active defects in ZnO is an important underpinning topic, because a thorough understanding of such defects is key to realising applications of this material. I will discuss a subset of recent work on ZnO, concentrating on photoluminescence defect studies in both nanostructured and bulk ZnO, including (i) radioactive isotope implantation studies (Fig. 1) [1] and other studies of I-line and other near bandedge features and (ii) studies of the nature of the surface exciton feature (Fig. 2) [2, 3].

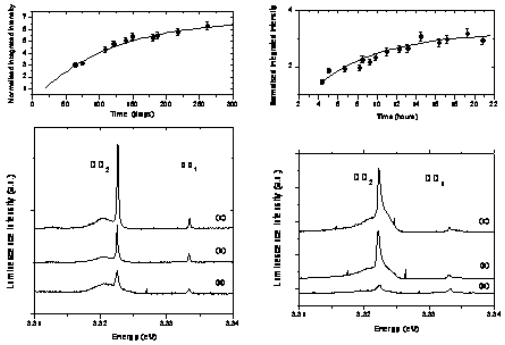

Fig. 1: Behaviour of DD2 (3.322 eV) near bandedge PL feature in ZnO following radioactive isotope implantations of 73As and 73Ga into ZnO single crystals [1].

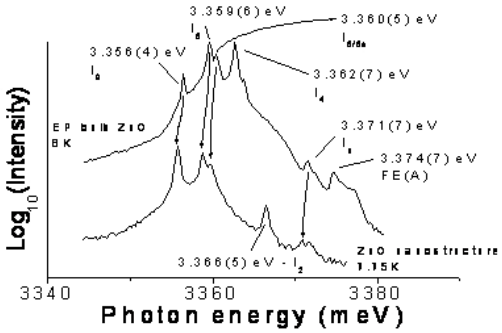

Fig. 2: Surface exciton (SX) near bandedge PL feature (3.3665 eV) in ZnO nanostructures [2].

References

[1] Karl Johnston, Martin O. Henry, Deirdre McCabe, Enda McGlynn, Marc Dietrich, Eduardo Alves, and Matthew Xia, Phys. Rev. B 73, article# 165212 (2006).

[2] J. Grabowska, A. Meaney, K. K. Nanda, J.-P. Mosnier, M. O. Henry, J.-R. Duclère, and E. McGlynn, Phys. Rev. B 71, article# 115439 (2005).

Nano-indentation study of femtosecond laser induced periodic surface structures on dielectrics and semiconductors

M. Rohloff[1,2*], A. Richter[1], K. Dasari[2], R. Hertmanowski[3], S.K. Das[2], A. Rosenfeld[2], and R. Grunwald[2]

** corresponding author : mrohloff@mbi-berlin.de*

[1] *Department of Engineering Physics, Technical University of Applied Sciences, Wildau, Bahnhofstrassse 1, 15745 Wildau, Germany*
[2] *Max Born Institute for Nonlinear Optics and Short Pulse Spectroscopy, Max-Born-Straße 2 A, 12489 Berlin, Germany*
[3] *Institute of Physics, Poznan University of Technology, 60-695 Poznan´, ul. Nieszawska 13 A, Poland*

Introduction

The generation of nanoscale LIPSS (Laser Induced Periodic Surface Structures) is based on the nonlinear interaction of intense short laser pulses with the material surface. Such structures can find their application in different technological fields [1]. Generally, the mechanical properties are changed during laser processing [2]. Nano-indentation studies of various dielectrics and semiconductors (TiO_2, c-SiO_2, a-SiO_2 and c-Si) were performed to study the mechanical properties of low (LSFL) and high spatial frequency (HSFL) LIPSS obtained by femtosecond laser irradiation of these materials.

Experimental details

The LIPPS were created by focusing 150 fs laser pulses (central wavelength 800 nm, repetition rate *Rp* of the laser system 150 Hz or 1000 Hz) onto the sample by either single pulses or double pulse sequences. In single pulse experiments, one laser pulse of definite energy beats the substrate in one time period $T = 1/Rp$. In double pulse experiments, on the other hand, two laser pulses of nearly equal energy reach to the substrate during one time period. The separation Δt between both peaks of the double pulses could be varied between 0 to 167 ps. Four different materials TiO_2, c-SiO_2, a-SiO_2 and c-Si were used for this study. LIPSS in one of the materials (TiO_2) was generated by femtosecond pulses at 400 nm (SHG).
To determine the nanoscale hardness, a modified AFM set-up was applied. The nanoindenter (Triboscope, Hysitron) can generate a maximum load of 10 mN. The indentation tip was a diamond 90° cube corner indenter. The tip was blunted with a radius of 650 nm. The indenter geometry was chosen to find a compromise between technical stability of the tip and the size of the nanostructures. The multi-indentation (MI) process was adopted in order to get information on mechanical properties in different depths according to the number of indents (4 or 12). The load was varied from 0.6 to 4 mN. For the lower range of load smaller than 1 mN the contact depth was found to be ~ 20-30 nm. As these values of depths are around 10-20% of the height of the ripples, the major part pf the extracted information stems from the ripples themselves. For higher ranges of applied load, however, the contact depths increases and information from both, ripples and bulk material, are obtained.

Results and discussion

The typical crossed LIPSS generated by fs double pulse sequences and their load-displacement data for 1 mN load for the c-SiO_2 are shown in Figure 1. Similar data for 3 mN load for TiO_2 (rutile) are plotted in Figure 2. The values for the final depth of contact impression after unloading (h_f) and contact depth (h_c) obtained from these graphs were used for calculating hardness and reduced indentation modulus following the *Oliver-Pharr*-method [3]. The average values of hardness H and modulus E_{red} in the c-SiO_2 were found to be 3.35 GPa and 64.2 GPa, respectively. These values amount to 35% and 60% of the bulk (i.e. unstructured) c-SiO_2.

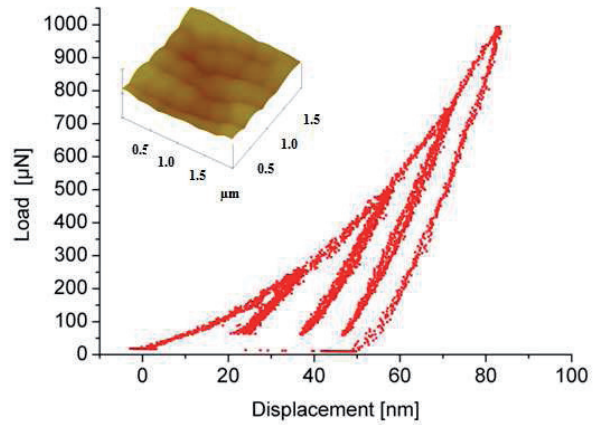

Figure 1: Load displacement curve of 4 multi-indents in crossed LIPSS in c-SiO_2 (period of HSFL ~ 350 nm, period of LSFL ~ 500 nm); inset: corresponding AFM-picture of the ripples.

A reduction in hardness and Young's modulus was also found in crossed LIPSS on a-SiO_2 and low spatial frequency LIPSS on c-Si and TiO_2 (Table I). This reduction in measured values of H and E_{red} is obviously caused by geometrical effects.

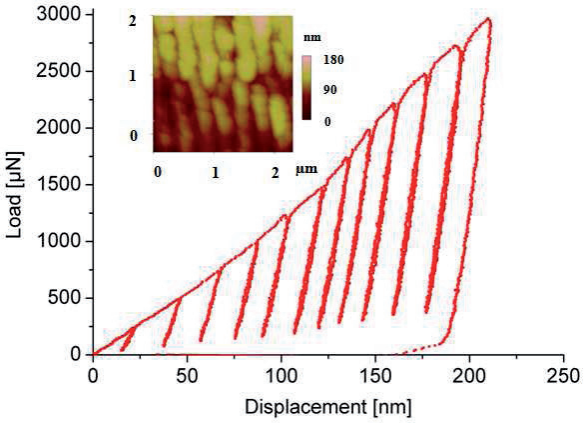

Figure 2: Load displacement curve for 12 multi-indents in LSFL (period about 300 nm) in rutile-type TiO_2; inset: corresponding AFM-picture of the LIPSS.

For both phases of SiO_2, a large reduction (over 60%) in hardness was measured. This could be caused by the coexistence of both HSFL and LSFL ripples in crossed orientation. For other materials (Si and TiO_2) where only one type of ripple structures appears, the reduction was found to be significantly less (Table I). At least, these observations further confirm our assumptions. To summarize, the results indicate a relationship between the size of the structures and their mechanical properties. This promises new approaches to control tribological and related mechanical parameters of functional materials on nanoscale via nonlinear, self-organized structuring processes based on ultrafast laser excitation.

Table I

Material	Type of LIPSS	Period of LIPSS (nm)	Load L (mN)	H (GPa) (% reduction w.r.t. reference)	E_{red} (GPa) (% reduction w.r.t. reference)
c-SiO_2	HSFL+LSFL	300-550	1	3.35 (65.0)	64.20 (40.0)
a-SiO_2	HSFL+LSFL	300-550	1	2.46 (63.9)	44.82 (28.2)
c-Si	melting (>LSFL)	1000-1500	1	5.70 (39.2)	89.30 (18.5)
TiO_2	LSFL	300	3	11.00 (35.3)	250.00 (3.8)

References

[1] A. Y. Vorobyev and C. Guo, Appl. Phys. Lett. **92**, 041914 (2008).
[2] J. Kim, J. Kim, and M. Lee, Surface & Coatings Technology **205,** 372 (2010).
[3] W.C. Oliver and G.M. Pharr, J. Mat. Res. **7**, 15 (2010).

Ultrafast electron dynamics in ZnO/Si micro-cones

E. Magoulakis, E.L. Papadopoulou, E. Stratakis, C. Fotakis and P.A. Loukakos

Foundation for Research and Technology—Hellas, Institute of Electronic Structure and Laser, P.O. Box 1385, 71110 Heraklion, Greece

A comparative study of the ultrafast dynamics in ZnO thin films deposited on flat Si substrates (Fig. 1a) and on Si micro-cones (Fig. 1b-d) following ultrashort laser excitation has been carried out using time-resolved optical spectroscopy[1]. By monitoring the transient band gap renormalization induced by nonlinearly excited carriers it is found that fast electron scattering and trapping occurs more efficiently in the microcones as compared to the flat films (Fig.2). From Fig 1, we find three structural differences that can be responsible for this acceleration: a) macroscopic conical shape, b) micrometer-sized protrusions along the cone surface and c) possibly film thickness variation from the top of the cones to their base. Additional measurements on films with different thicknesses (Fig. 3) and different cone sizes (Fig. 4) show that the measured signal is independent of both. Therefore, the enhanced trapping efficiency is attributed to the defects and imperfections that are introduced by the increased surface roughness due to the conical shape.

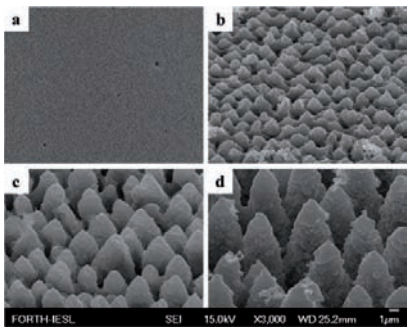

Figure 1: FE-SEM images of (**a**) ZnO film on a flat Si substrate. (**b**–**d**) ZnO on micro-conical Si substrates with various sizes and aspect ratios of the cones: (1.6:1.5), (4.7:3.6) and (9.9:6.0) respectively

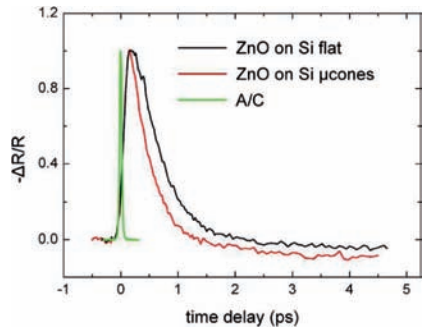

Figure2: Time-resolved reflectivity changes of thin ZnO films on flat Si (*black*) and on Si micro-cones (μcones) (*red*). Autocorrelation (*A/C*) of the fundamental laser pulses is also displayed for comparison purposes (*green*)

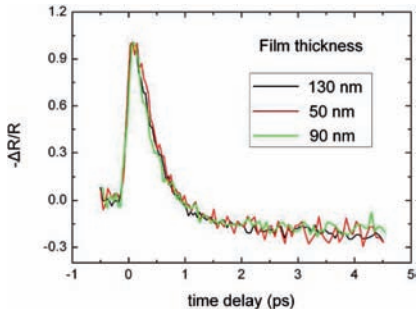

Figure 3: Time-resolved reflectivity changes for various thicknesses of thin films of ZnO on flat Si substrates.

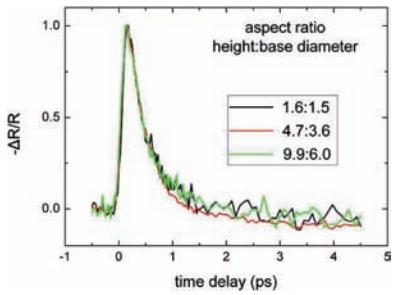

Figure 4: Time-resolved reflectivity changes for thin ZnO films on microconical Si substrates with varying sizes and aspect ratios (height : base diameter)

[1] E. Magoulakis et al, Appl. Phys. A **98**, 701 (2010).

Author Index

Page

Abel, B. 25
Albrecht, G. 39
Alves, E. 41
Andriotis, A. 30
Bansen, R. 40
Beresna, M. 14
Bestehorn, M. 13
Biswas, M. 41
Bock, M. 38
Boeck, T. 40
Bonse, J.O. 17, 18
Bounhalli, M. 13
Bormann, R. 23
Brintakis, C. 30
Bublitz, S. 32
Burger, S. 27
Cerullo, G. 20
Cho, W.B. 28
Choi, S.Y. 28
Cornet, A. 33
Coronado, E.A. 33
Das, S.K. 17, 38, 42/43
Dasari, K. 42/43
Dietrich, M. 41
Döring, S. 16
Duwe, M. 25
Farsari, M. 21, 37
Fotakis, C. 21, 37, 44
Gaidukeviciute, A. 21
Gecevičius, M. 14
Giessen, H. 22, 39
Goñi, A.R. 33
Gray, D. 21
Griebner, U. 28
Grunwald, R. 17, 38, 42/43
Güell, F. 33
Gulde, M. 23
Hashida, M. 10,11, 36
Henry, M.O. 41
Hentschel, M. 22
Herrmann, J. 24
Hertmanowski, R. 42
Hughes, G. 41
Höhm, S. 18

Page

Huisken, F. 32
Husakou, A. 24
Ikuta, Y. 10, 11, 36
Johnston, K. 41
Kabouraki, E.A. 21, 37
Kanaras, A.G. 30
Kazansky, P. G. 14
Kim, K.-H. 24
Kim, K. 28
Kitamura, K. 26
Kityk, I. 31
Kostopoulou, A. 30
Krüger, J. 18
Kühn, S. 34
Kumar, K 41
Lammers, M. 20
Lappas, A. 30
Leipold, D. 26
Lienau, C. 20, 26
Lippitz, M. 22
Liu, Y. 25
Loukakos, P.A. 30, 44
Magoulakis, E. 30, 44
Maiuri, M. 20
Manzoni, C. 20
Maschek, M. 26
Miyasaka, Y. 10, 11, 36
Metzger, B. 39
McCabe, D. 41
McGlynn, E. 41
Morante, J.R. 33
Mühlig, Ch. 32
Muth, M. 13
Nolte, S. 16
Ohtsu, M. 26
Ossó, J.O. 33
Paa, W. 32
Papadopoulou, E.L. 44
Pérez, L.A. 33
Petrov, V. 28
Pfuch, A. 17, 38
Pomraenke, R. 20
Potrick, K. 32
Purlys, V. 21

Author Index

Page

Reif, J. 13
Richter, A. 42
Richter, S. 16
Rohloff, M. 18, 42
Ropers, C. 23, 25
Rosenfeld, A. 17,18, 42/43
Rotermund, F. 28
Runge, E. 26
Sakabe, S. 10, 11, 36
Sakellari, I. 21, 37
Schmidt, A. 28
Schmidt, S. 26
Schmidt, T. 32
Schmidtbauer, J. 40
Schramm, H.P. 40
Schwanke, C. 38
Seeber, W. 17, 38
Siefermann, K.R. 25
Silies, M. 26
Sivis, M. 25
Steinmann, A. 39
Steinmeyer, G. 28
Stratakis, E 44
Teubner, T. 40
Tokita, S. 10, 11, 6
Tünnermann, A. 16
Utikal, T. 22
Vamvakaki, M. 21, 37
Varlamova, O. 13
Varlamov, S. 13
Vasa, P. 20
Wang, W. 20
Weismann, A. 23
Xia, M. 41
Yalunin, S.V. 23
Yatsui, T. 26
Yeom, D.-I. 28

(Speakers in bold)

Max-Born-Institute

for Nonlinear Optics and Short-Pulse Spectroscopy

Max Born

The name “Max-Born-Institute” is devoted to one of the most important pioneers of modern physics. Max Born received the Nobelprize in physics in 1954 (together with W. Bothe) "for his fundamental research in quantum mechanics, especially for his statistical interpretation of the wavefunction". More about Max Born can be found on our website under „about MBI“.

Mission

The MBI conducts basic research in the field of nonlinear optics and ultrafast dynamics of the interaction of light with matter and pursues applications that emerge from this research. It develops and uses ultrafast and ultra-intense lasers and laser-driven short-pulse light sources in a broad spectral range in combination with methods of nonlinear spectroscopy.
With its research the MBI fulfills a nationwide mission and is an integral part of the international science community. The MBI is involved in a large number and variety of cooperative research projects with universities, other research institutions and industrial partners.

Guest Program

In addition, the MBI also offers to external guest scientists to use its research capacities and the available know-how of the institute in the framework of an active guest program. More information can be obtained from the Directors, Prof. Marc Vrakking, Prof. Wolfgang Sandner and Prof. Thomas Elsässer.
Specifically the MBI managed (Prof. W. Sandner) and coordinated European Network „Laserlab Europe“ is of particular relevance with respect to the guest activities at the MBI.

Research structure and organizational structure

The research structure of the Max-Born-Institute comprises 10 research projects and two infrastructure projects, organized in 4 focus areas. Complementary to this, the organizational structure with 3 research divisions (each with 3 departments) defines the key fields of scientific competence of MBI-scientists and the corresponding scientific equipment.

Max-Born-Institute

The Leibniz Institute for Crystal Growth

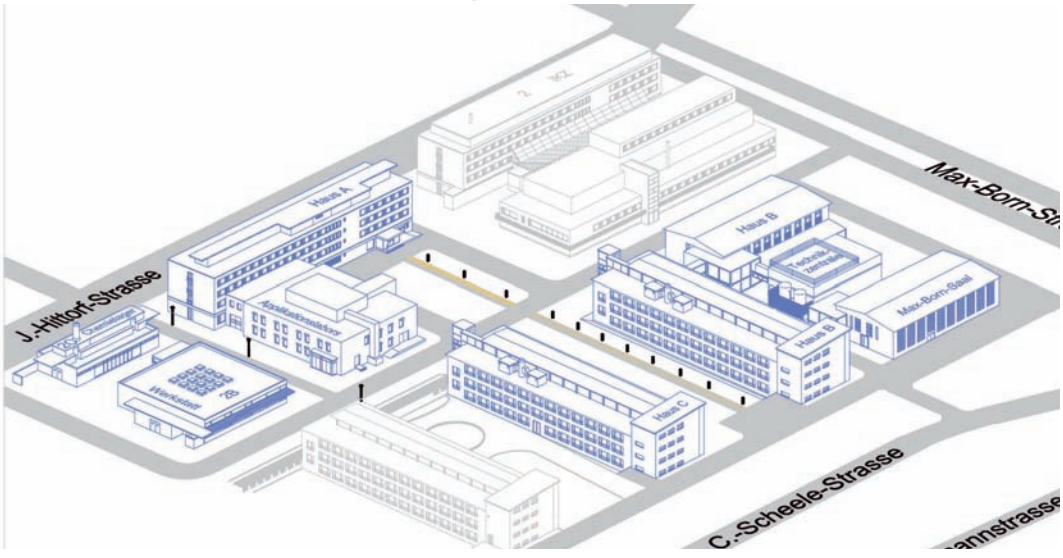

Notes